



## Research

# Analysis of urban expansion and its impact on temperature utilising remote sensing and GIS techniques in the Accra Metropolis in Ghana (1986–2022)



Bernard Fosu Frimpong<sup>1</sup> · Addo Koranteng<sup>2</sup> · Fosu Senior Opoku<sup>3</sup>

Received: 20 April 2023 / Accepted: 11 July 2023

Published online: 31 July 2023

© The Author(s) 2023 **OPEN**

## Abstract

The Accra Metropolis of Ghana has experienced rapid urban expansion over the past decades. Agricultural and forestlands have been transformed into urban/built-up areas. This study analysed urban expansion and its relationship with the temperature of Accra from 1986 to 2022. Multi-source datasets such as remote sensing (RS) and other ancillary data were utilised. Land use land cover (LULC) maps were produced employing the random forests classifier. Land surface temperature (LST) and selected d(RS) Indices were extracted. Regression techniques assessed the interplay between LST and remote sensing indices. The LULC maps revealed increasing trends in the urban/built-up areas at the expense of the other LULC types. The analysis from the LST and the RS indices revealed a direct relationship between temperature and urban/built-up areas and an inverse relationship between temperature and vegetation. Thus, spatial urban expansion has modified the urban temperature of Accra. The integrated utilisation of RS and GIS demonstrated to be an efficient approach for analysing and monitoring urban expansion and its relationship with temperature.

## Article Highlights

- Urban expansion has led to the conversion of agricultural and forestlands into urban areas in Accra, Ghana.
- There is a direct relationship between temperature and urban/built-up areas.
- The adopted techniques proved effective in analysing and monitoring urban expansion and its impact on temperature.

**Keywords** Urban expansion · Change detection · Land use land cover · Regression · Remote sensing · Temperature

## 1 Introduction

The population of the world is projected to reach 8.5 billion inhabitants in 2030 [1]. It has also been forecasted that an additional 2 billion people to be added to the world,

and 1.05 billion (52%) may come from sub-Saharan countries [1]. Urbanisation is a global phenomenon that has significant implications for the environment, particularly in relation to temperature dynamics within urban areas [2]. Urbanisation is the rise in both population and spatial

✉ Bernard Fosu Frimpong, frimpber@gmail.com; Addo Koranteng, addo.koranteng@kstu.edu.gh; Fosu Senior Opoku, opokuf1@my.smccd.edu | <sup>1</sup>Department of Hydrology, Brandenburg University of Technology, Platz der Deutschen Einheit 1, 03046 Cottbus, Germany. <sup>2</sup>Institute of Research, Innovation and Development, Kumasi Technical University, Kumasi, Ghana. <sup>3</sup>College of San Mateo, 1700 W Hillside Blvd, San Mateo, CA 94402, USA.



expansion in urban areas [3]. It is a complex network of processes that leads to the transformation of the environment [4] and a multifaceted phenomenon encompassing demographic, ecological, sociological, and economic aspects [5]. Urbanisation results in the concentration of populations within urban areas and possesses the capacity to either stimulate or hinder the growth and advancement of these areas [6].

The magnitude of global urbanisation is remarkable, with the United Nations projecting that by 2050, nearly two-thirds of the world's population will reside in urban areas [4]. The fastest rate of urbanisation is found in Africa and it is projected that more than half of the continent's inhabitants will be living in urban areas [7]. Urbanisation has positive sides that include human development, economic rise and reduction in the alleviation of poverty but it has been a major challenge for African countries including Ghana [8].

Many portions of Ghana have been classified as urban. These areas have a population of 5000 or more inhabitants [9]. In Ghana, 56.7% of the population live in urban/built-up areas in 2021 [10]. Ghana's total land size is estimated at 238,539 square kilometres [11]; the urban/built-up areas covered 1460 square kilometres (0.6%) and 3836 square kilometres (1.6%) in 1975 and 2013, respectively, of the total area of Ghana [12]. Most cities in Ghana were founded for economic reasons during the pre-colonial era. In addition, a chain of coastal cities, primarily Elmina, Cape Coast and Accra (from 1860 to 1905), was established for trade reasons [13].

Cities in Ghana have increased both in population and areal extent [14, 15] and thus rapid spatial urban expansion has become a key feature of the major urbanised centres in Ghana [16–18]. The Accra metropolis is regarded as the most populous city in Ghana with 2,218,487 inhabitants [10]. It has experienced a lot of land use land cover changes (LULCC) due to urbanisation [16, 17]. Mapping using satellite imagery has led to a deeper understanding of the dynamics in urban/built-up areas [19] at the global level [20]; regional level [21] and city level utilising remote sensing techniques [22].

Remote Sensing (RS) is the art of obtaining observations from a phenomenon utilising instrument-based techniques [23]. It has been utilised to obtain meaningful data from the electromagnetic spectrum and has enabled features to be measured in urban/built-up areas [24]. Geographic Information Systems (GIS) and Remote Sensing (RS) have been used to generate Land Use Land Cover (LULC) maps from Landsat satellite images in various cities in Ghana [18, 22, 25–28] with results indicating a high transformation of other LULC classes especially, agricultural and forestlands into urban/built-up areas and has adversely impacted temperature [22, 27, 29]. These

techniques have been adopted for both retrospective [28] and prospective studies [22].

Future land use land cover modelling techniques have been adopted around the world; in Florida, USA [30]; Beijing, China [31]; Daqahlia Governate, Egypt [32]; Abuja, Nigeria [33]; Kumasi [22] & Greater Accra Metropolitan Area [26] in Ghana. The Artificial Neural Network (ANN) based cellular automation technique was adopted for future modelling in several studies [34, 35]. The Cellular Automata – Markov chain [26, 36]; the CLUE-S model with the Markov model [31]; and the use of the Markov chain model [22, 37]. The results from the works of [22, 26, 37] predicted increases in the urban/built-up areas for the predicted years of the study areas investigated.

Seminal studies have documented the relationship between LULC and Land Surface Temperature (LST) worldwide [38–41]. In Ghana, the relationship between LULC and LST has been studied in the Sekondi-Takoradi Metropolis and revealed that LST was higher in the urban/built-up areas than in the city's non-urban/built-up areas. The study concluded that there was an indirect relationship between the Normalised Difference Vegetation Index (NDVI) and LST [42]. The works of [17] and [43] investigated the extent of warming trends in Tarkwa and the Greater Accra Region respectively. Results revealed that urban/built-up areas yielded increasing warming trends in both study areas.

Ordinary Least Squares (OLS) regression is regarded as a straightforward technique and generates an equation to represent a process [44]. It has been used to determine the impact of biophysical parameters on LST [45–47]. The Geographically Weighted Regression (GWR) is also a linear regression used to model spatially varying relationships. It constructs individual equations for each component in the dataset [48]. The correlation between LULC and land surface temperature [49]; the relationship between LST and NDVI, Normalised Difference Built-up Index (NDBI) [50]; assess the spatial correlation between temperature and environmental factors [51]. Results have revealed a negative relationship between LST and NDVI and a positive relationship between LST and NDBI [50, 51].

Previous literature have characterised the magnitude and the spatial coverage in Ghana. The research of [52] used a short duration of 12 years (2005–2017) to investigate the relationship between Land Use Land Cover (LULC) and Land Surface Temperature (LST) in Accra. It provided limited insights into the magnitude, intensity and spatial coverage in the selected cities. The research of [53] investigated rising temperatures resulting from urbanisation in Accra. However, the focus was not hinged on LULCC and spatial extent. The scientific work of [17] provided insights into increasing temperatures in the Greater Accra Region but put less focus on the nexus between LST and

(Normalised Difference Vegetation Index (NDVI) and Normalised Difference Built-up Index (NDBI) which are good indicators of urban warming within an area according to the research of [54, 55].

Again, the studies of [56–58] focused on the characterisation and quantification of urban/built-up areas in Ghana whilst the research of [59] focused on environmental pressures exerted by urban expansion and introduced the spatial transformation of the various land cover classes in the metropolitan areas in Ghana. Most reviewed studies in Ghana have not focussed on the increasing temperatures resulting from spatial urban expansion [26, 43, 60]. Works cited used the traditional classifier, especially, the Maximum Likelihood Classifier which is based on probability [16, 17, 26] whilst the advent of state of the art, Machine Learning Algorithms has improved image classification [61–63] but little attention has been on the utilisation of machine learning algorithms for satellite image classification in Ghana.

In our research, we seek to fill this knowledge gap by utilising RS images from 1986 to 2022 to analyse the regression between LST and (NDVI and NDBI) not addressed in previous research in the Accra Metropolis. Moreover, the research will provide an insightful comprehension of spatial urban expansion in the Accra Metropolis in Ghana.

## 2 Materials and methods

### 2.1 Study area

Accra acts simultaneously as the capital of the Greater Accra Region and Ghana. The capital is in the South-Eastern portion of the coast of the Gulf of Guinea. The centre of the Metropolis is coordinated as 5.56°, -0.21°. The average monthly temperature ranges from 24.7 to 33 °C. The Local Government Act, 1993 (Act 462) and the Legislative Instrument (LI) 1615 established the Accra Metropolitan Assembly (AMA). The AMA consists of the Ablekuma (North, South and Central), Ayawaso (East, West and Central), Okaikoi (North and South), Ashiedu Keteke, Osu Klottey and Kpeshie (Fig. 1).

### 2.2 Dataset

The essential Landsat satellite imagery with a cloud cover of less than 10% was downloaded, acquired and assembled as described in Table 1.

The supplementary dataset utilised were the Open Street Map (OSM), World Topographic Map (WTM) and the World Street Maps (WSM). The OSM road network dataset

was obtained from Geofabrik's website. The WTM and the WSM were Base maps in the ArcGIS software.

The generalised methodology adopted for the overall of this study is shown in Fig. 2. The entire workflow is segmented into two portions;

- The utilisation of satellite images for LULC changes and accuracy assessment, urban modelling for 2030 and urban expansion analysis
- The usage of satellite images for remote sensing indices and LST analysis (Fig. 2)

### 2.3 Satellite image processing and classification

Landsat images were resampled utilising the Nearest Neighbour technique. The Nearest Neighbour (NN) resampling technique was utilised. The original values of the original image are preserved in comparison to other techniques [64]. The satellite images were projected to the World Geodetic System (WGS) 84, Universal Transverse Mercator (UTM) Zone 30 N and the Ghana Datum War Office. The area of interest i.e. Accra Metropolis was extracted from the World Topographical Map and the Landsat images for onward processing. The different bands (excluding the thermal and panchromatic bands) were stacked to form a composite band.

According to [65], four LULC groups were classified for the selected Landsat images regarding earlier works on LULC classification in Accra [16]. The LULC classes were urban/built-up areas, agricultural, forestlands and water. A concise description of the classes is illustrated in Table 2.

The classification technique utilised was supervised classification. It was utilised for identifying, classifying and evaluating LULC groups. The assigning of pixels to their chosen classes was done using the Random Forest technique. The Random Forest algorithm is utilised to classify satellite images through the creation of trees [66]. This algorithm offers improved accuracy in classification and reduced computational time compared to other methods [67, 68]. The input data consisted of spectral bands, and the output was the dominant land use and land cover (LULC) class determined by majority voting. Each tree operated independently, enabling simultaneous training and testing processes. The technique is not limited by statistical assumptions was thus the reason for choosing the technique [66].

### 2.4 Assessment of the accuracy of the classified satellite images

The training areas of the various LULC types were assessed for the 2022 Landsat image. The ground control points

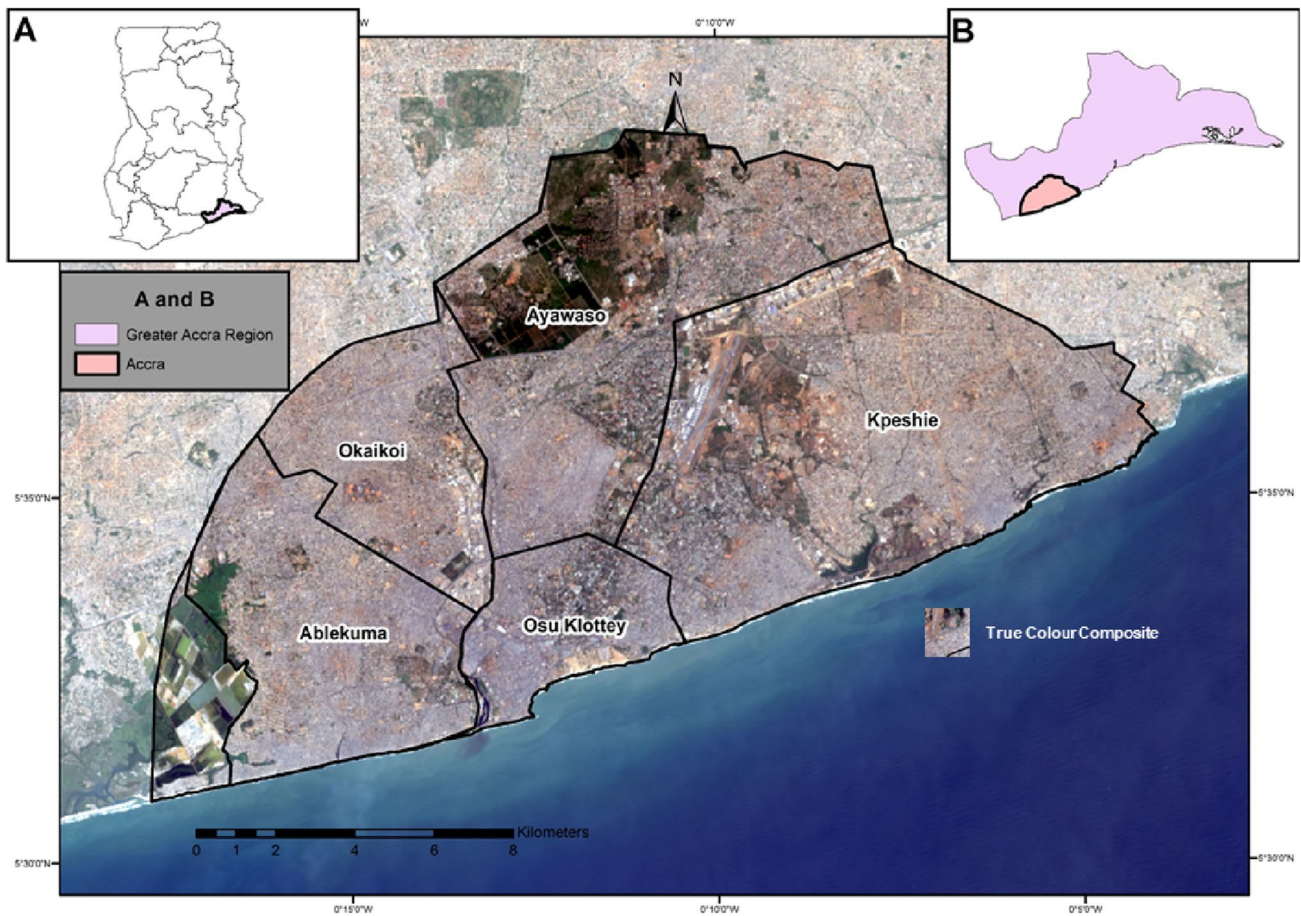


**Fig. 1** Map showing the study area (A = Map of Ghana showing the Greater Accra Region; B = Map of Greater Accra region showing the Accra Metropolis)

**Table 1** Datasets used in the research

Satellite	Date of Acquisition	Number of Bands	Resolution (m)
<b>(a) Landsat Series</b>			
Thematic Mapper (TM)—5	22.12.1986	7	30/120
Enhanced Thematic Mapper (ETM+) – 7	12.02.2003	8	30/15/60
Operational Land Imager (OLI/TIRS) – 8	06.12.2015	11	30/15/100
Operational Land Imager (OLI/TIRS) – 8	25.12.2022	11	30/15/100

were evaluated and validated utilising the GPS etrex 64 s. The fieldwork for validating the classified image of 2022 was done in January 2023 for ten days. The field visit was undertaken in the dry season since the Landsat images were also obtained during the same period. This made it suitable to correlate satellite images to the ground features. The equalised stratified random sampling technique was used for the generation of the field points because it created the same number of random points for each LULC class. These ground control points were 200 sample points for the four LULC classes (i.e.) 50 samples for each LULC

class. The supplementary map datasets aided in the identification of the different LULC groups.

### 2.5 Land use land cover modelling and validation for 2030

The methodological flow of the adopted techniques for land use land cover modelling and validation is illustrated in Fig. 3.

Before modelling and validation, the conditions to be met are carried out and these are; initial checks to ensure

**Fig. 2** Methodological framework adopted for this research

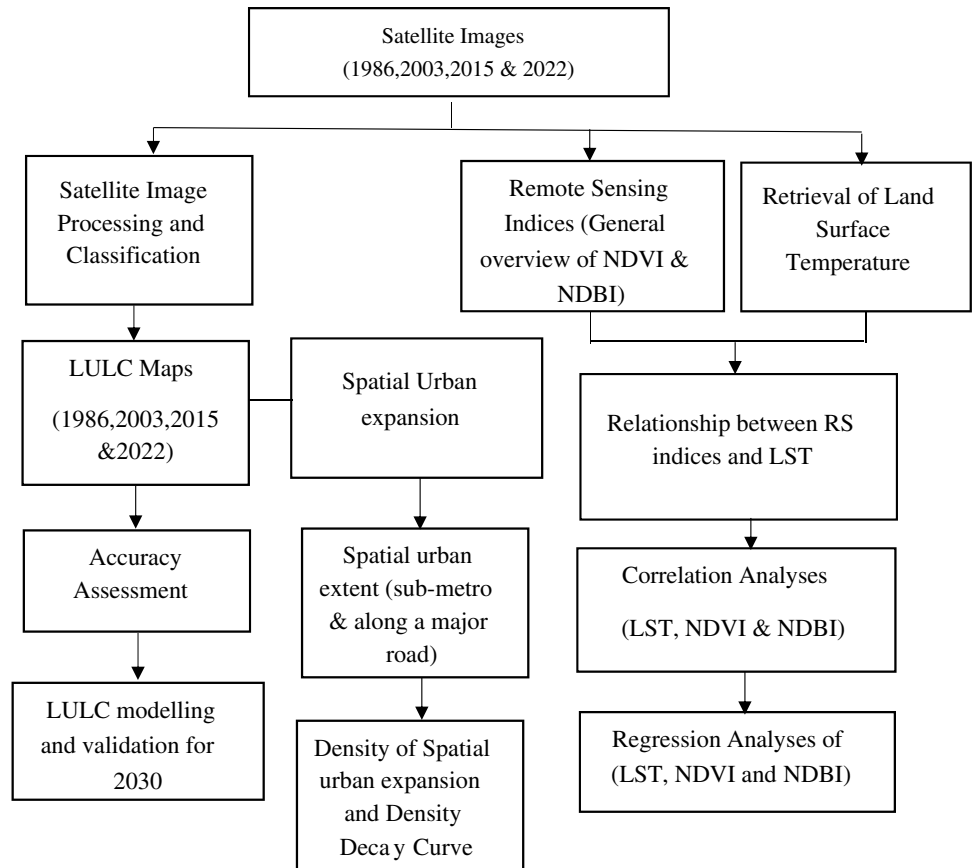


**Table 2** LULC classes

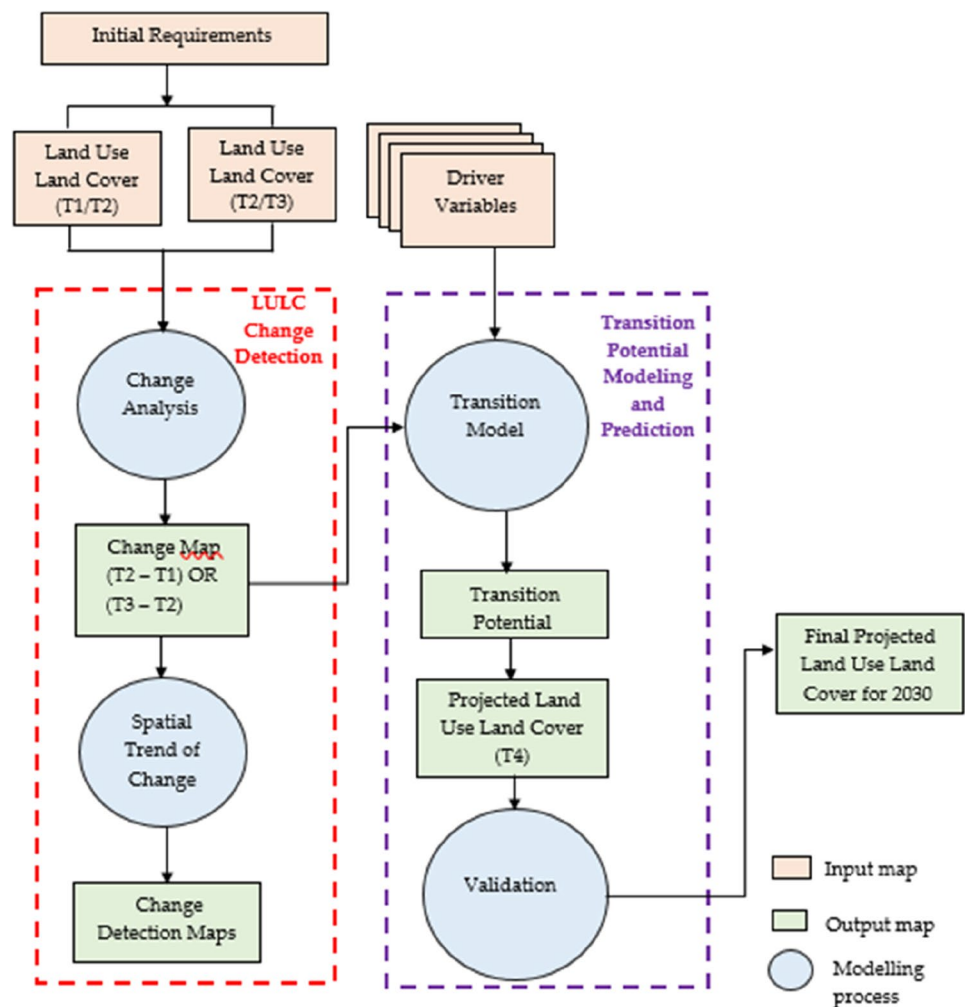
LULC category	Description
Urban / Built-up	Residential Commercial Industrial Power and communications facilities Institutions Highways and Transportation Lands with exposed soil surface
Agricultural Lands	Cropland Horticultural Areas Pasture
Forestlands	Mixed Forestlands: short canopy trees of about 5–10 m high with a thin occurrence of some emergent trees
Water	Rivers Streams Lakes Lagoons Wetlands

that the temporal satellite images were harmonised, had the same spatial features, legend and the same consistent categories and finally, the backgrounds of the satellite images had the same value of zero.

The temporal images of 2003 and 2015 were designated as **t1** and **t2** respectively. Both temporal images were used as the base maps. The first step was the change analysis. The ‘from—to’ identified were the transitions from one land cover type to another. The analysis of the prediction was achieved by utilising an aggregate of empirically transitioned sub-models. The driving variables utilised in this research were; Slope, Elevation, Distance to urban/built-up areas and Distance to major roads.

The driver variables were considered the main variables that influenced spatial urban expansion. The selection of the driver variables was based on the review of initial studies [25, 69]. The slope and elevation were used to account for the geophysical factors. The distance drivers indicated the nearness of pixels to forces that act as motivation for spatial urban expansion. In 2003, the distance to urban/built-up areas was set as a dynamic variable. The distance to the urban variable indicated the proximity of a pixel to existing urban/built-up areas in 2015. The modelling of the distance to urban/built-up areas was set up as a dynamic variable because the distance of urban pixels changes with time.

**Fig. 3** Flowchart for future LULC modeling



The Multi-Layer Perceptron handles multiple transitions at a time. The neural network was trained to build a model utilising the information from the data such that the network could hypothesise and forecast the outputs. The error in the network was minimised by adjusting the weights between the nodes (utilising a proportion of the input data), and utilising the backpropagation algorithm. After iterations, the calculation of the error across the neural network was executed. The model was trained utilising sample pixels in the two LULC maps that experienced changes from one land use to another, as well as pixels that remained unchanged. The sample size was set to the least number of pixels that changed from one LULC type to another by default. The pixels were divided into two groups, one for training the model and the other for testing or validating the model's accuracy. The Markov Chain Analysis was utilised to model the quantitative changes in each transition for the projected year (2030). The potential maps generated were utilised to forecast the future scenario of 2022. The forecasted map with the same LULC classes as the input maps were produced.

Validation enabled the determination of the quality of the predicted maps of 2022 compared to the real 2022 LULC maps. Visual and statistical approaches were used to validate the models (Pontius & Chen, 2006). This resulted in a map consisting of four main categories:

- i. 'Hits' meant the changes predicted by the model were correct.
- ii. 'False alarms' meant the model predicted changes but no changes occurred.
- iii. 'Misses' signified that the model predicted no changes, but changes happened.
- iv. 'Null success' meant areas the model predicted no changes and no changes occurred.

Finally, after the verification, the model's predictive potential was performed between (2003 and 2015). Then, the simulation was done to predict the LULC map of 2022 utilising (2003 and 2015 LULC maps) as the base maps. The entire procedure was repeated to obtain the projected map of 2030.

## 2.6 Remote sensing indices

The NDVI is the most widely used remotely sensed vegetation index [70] and thus was extracted for this study. It is among the extensively used vegetation indices to communicate vegetation information [71]. The NDVI reveals the greenness of an area of interest due to its higher sensitivity in the presence of vegetation [72]. NDBI was used to extract urban/built-up areas from the satellite imagery. It indicated the intensity of development and impervious surfaces of urban/built-up areas. Both indices are indicators of Urban Heat Islands (UHIs) effects by determining their relationships with LST [55]. Thus, the rationale for analysing NDVI, NDBI and LST in this research. We adopted a pragmatic approach by using each one of the vegetation indices and built-up indices despite the variety of indices available. This enabled a precise investigation into the study area utilising the RS indices.

The Near Infra-Red (NIR) and the Red (R) bands were utilised for the computation of NDVI as;

$$NDVI = \frac{NIR - R}{NIR + R} \quad (1)$$

The NDBI was computed using the Short Wave Infra-Red (SWIR) and the NIR bands as shown in the equation:

$$NDBI = \frac{SWIR - NIR}{SWIR + NIR} \quad (2)$$

## 2.7 Retrieval of land surface temperature

To obtain the LST, the following computations were done. The thermal Digital Numbers (DN) were converted into spectral radiance using the Equation based on [73].

$$L_{\lambda} = \frac{L_{max\lambda} - L_{min\lambda}}{Q_{calmax} - Q_{calmin}}(DN - Q_{calmin}) + L_{min\lambda} \quad (3)$$

where:  $L_{\lambda}$  = Spectral Radiance,  $L_{max}$  = Spectral radiance of DN value 255,  $L_{min}$  = Spectral radiance of DN value 1,  $Q_{calmax}$  = Maximum numerical value of the image (retrieved from header file),  $Q_{calmin}$  = Minimum numerical value of the image (retrieved from header file).

For the Landsat 8 satellite image of 2015, computation into spectral radiance from DNs was done using the equation:

$$L_{\lambda} = M_L * Q_{cal} + A_L \quad (4)$$

where:  $L_{\lambda}$  = Spectral radiance ( $W / (m^2 * sr * \mu m)$ ),  $M_L$  = Radiance multiplicative scaling factor for the band (RADIANCE\_MULT\_BAND\_n from the metadata)

$A_L$  = Radiance additive scaling factor for the band (RADIANCE\_ADD\_BAND\_n from the metadata)

$Q_{cal}$  = Level 1 pixel value in DN [74].

However, the flow for the calculation of LST remained the same. Thus, the spectral radiance was then converted into brightness temperature using the equation:

$$T_{sat} = \frac{K_2}{\ln\left(\frac{K_1}{L_{\lambda}} + 1\right)} \quad (5)$$

where:  $T_{sat}$  = Brightness Temperature,  $L_{\lambda}$  = Spectral Radiance,  $K_1$  = Calibration constant 1 (607.76 for TM, 666.09 for ETM+ and 774.89 in Landsat 8 Band 10),  $K_2$  = Calibration constant 2 (1260.56 for TM, 1260.56 for ETM+ and 1321.08 in Landsat 8 Band 10)

Finally, the surface temperature was converted from Kelvin  $T_{sat}$  to Degrees Celsius  $T_c$  by applying the equation:

$$T_c = T_{sat} - 273 \quad (6)$$

The emissivity was calculated from the NDVI [75] by applying the equation:

$$\epsilon = 1.0094 + 0.047 \ln(NDVI) \quad (7)$$

hence, LST based on object reflectance using was calculated using the algorithm:

$$LST = \frac{T(^{\circ}C)}{(1 + (\lambda * T(^{\circ}C) / \rho) * \ln(\epsilon))} \quad (8)$$

where:  $T(^{\circ}C)$  = calculated brightness temperature,  $\lambda$  = Raw wavelength of emitted radiance,  $\rho = h * c / \sigma$  ( $1.4038 * 10^{-2} mk$ );  $\sigma$  = Stefan Boltzmann's constant;  $h$  = Plank's constant;  $c$  = light velocity.

## 2.8 Correlation analysis

The satellite images from the Landsat series were employed. It was used to provide a general overview of NDVI, NDBI and LST of the Accra metropolis. A total of 260,005 were generated using an approximated factor of 0.09. This optimum number of points (260,005) was used to determine the NDVI, NDBI and LST value for each point created. This was done to ascertain the correlation amongst them. Thus, the Accra metropolis with 23,400 ha was divided by the approximated factor (0.09) to obtain the total number of points.

## 2.9 Regression analyses of LST, NDVI and NDBI

Both global (Ordinary Least Squares) and local (Geographic Weighted Regression) were used to evaluate the relationships between LST, NDVI and NDBI.

### 2.9.1 Ordinary least squares

OLS based on the assumption that there are independent observations and thus fails to encompass the spatial dependence of the data when applied to geo-referenced data analysis [51].

The Ordinary Least Squares (OLS) was computed as;

$$Y = \lambda + \beta_1 X_1 + \beta_2 X_2 + \beta_3 X_3 \quad (9)$$

### 2.9.2 Efficiency Criteria for the OLS

The coefficient for each explanatory variable reflected the strength and relationship the explanatory variable has with the dependent variable. If the coefficient was positive, the relationship was positive and vice versa. The model performance was evaluated using the R-squared and the adjusted R-squared values. The values ranged from 0.0 to 1.0. It was regarded as an accurate measure of model performance [76].

The assessment of each explanatory variable was done using the Variance Inflation Factor (VIF). It measured multicollinearity. A high VIF value was an indication of high collinearity. Mostly, the VIF threshold was set at 7.5 [77]. The joint F-statistic and joint Wald statistic evaluated the statistical significance of the model. For a 95% confidence level, a p-value less than 0.05 indicated a statistically significant model [78].

The Koenker (BP) Statistic tested if the explanatory variable in the model had a consistent relationship with the dependent variable in geographical space. At a 95% confidence level, a p-value (probability) smaller than 0.05 indicated statistically significant heteroscedasticity and/or non-stationarity [78]. The evaluation of model bias was evaluated using the Jarque-Bera statistic that indicated whether the residuals were normally distributed. If the residuals were not normally distributed it implied that the model was biased [77]. The Akaike's Information Criterion (AICc) provided additional information on the model performance [78].

### 2.9.3 Geographic weighted regression

GWR used in this research was mathematically equated as;

$$y_i = a_0(u_i, v_i) + \sum_k a_k(u_i, v_i) x_{ik} + \sum_i i \quad (10)$$

where  $(u_i, v_i)$  represented the coordinates of the  $i$ -th point in space and  $a_k(u_i, v_i)$  was a realisation of the continuous function  $a_k(u, v)$  at the point  $i$  [79].

### 2.9.4 Efficiency criteria for GWR

The Bandwidth or Number of Neighbors was utilised for the local estimation and was regarded as the most essential parameter for GWR. The bandwidth was automatically generated as 205 neighbours [78]. The sum of the squared residuals in the model was the residual squares. The smaller the residual squares, the closer the fit of the GWR model to the observed data [78].

Effective Number reflected the trade-off between the variance of the fitted values and the bias in the coefficient estimates and was related to the choice of bandwidth [78]. Sigma was the value of the square root of the normalised residual sum of squares when the residual sum of squares was divided by the effective degrees of freedom of the residuals. Smaller values of this statistic were preferable. Sigma was used for AICc computations [78].

The AICc measured model performance and was useful for the comparison of different regression models. If the AICc values for the two models differ by more than 3, the model with the smaller AICc was regarded as better [78]. The R-squared and the Adjusted R-squared were measures of goodness of fit. Its value varied from 0.0 to 1.0 with higher values being preferable [76].

## 3 Results

### 3.1 Satellite image processing and Classification

The classified image of 1986 revealed that the urban/built-up areas began along the coast and spread upwards and outwards to the other portions of the Metropolis (Fig. 4). Again, most of the urban/built-up areas were close to the coastline (the southern boundary of the Metropolis). The forestlands were surrounded by a large number of agricultural lands generally in the northern parts of the city. The classified image of 2003 revealed dominance by urban/built-up areas. Most of the agricultural lands were gradually depleting. Moreover, in the classified image of 2015, a higher proportion of urban/built-up with agricultural lands decreasing was observed. The visual inspection indicated a rise in forestlands. The water environment visually appears to have maintained its shape throughout the study.

The urban/built-up areas dominated the other land cover types for the entire study. It covered more than half of the land size of Accra. The water environment occupied the smallest area. However, agricultural lands continued to diminish until the last year. There was a decrease from 1986 to 2003 for forestlands but a gradual increase was observed in 2015 (Fig. 4)



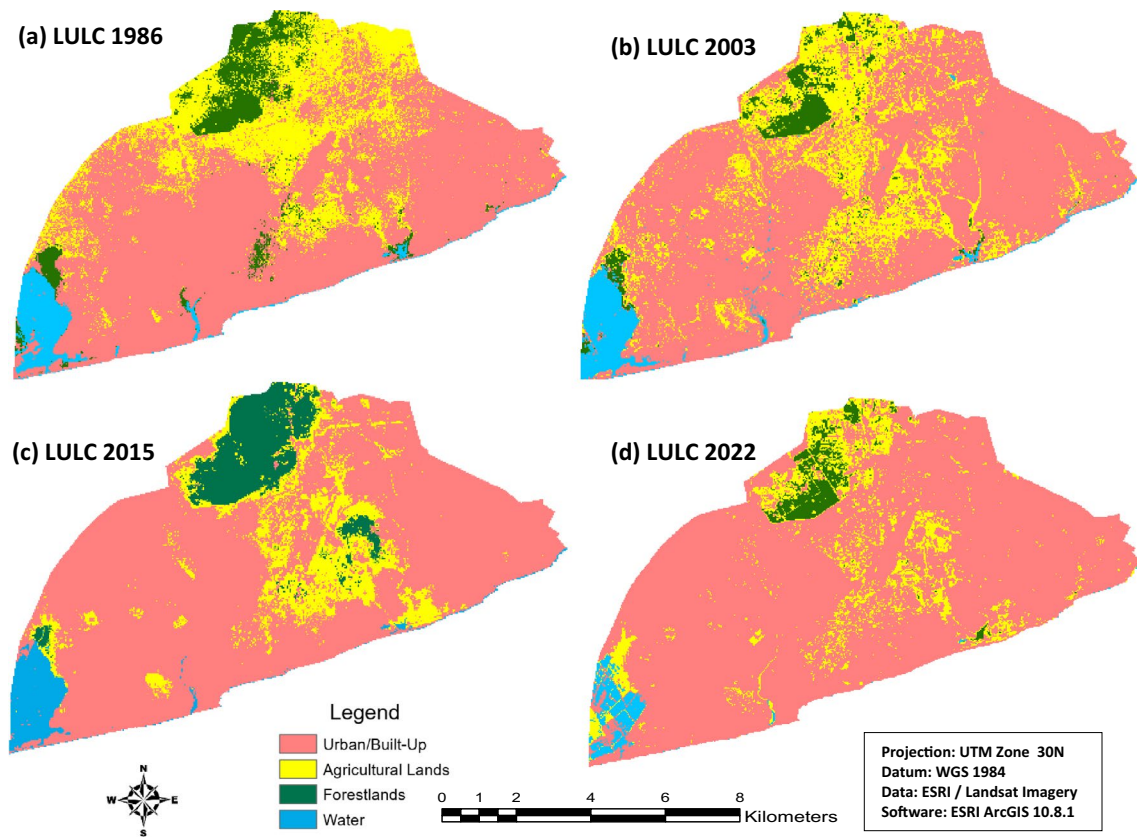


Fig. 4 LULC maps for Accra for the years 1986, 2003 and 2015

Similar patterns in the increasing trends in urban/built-up areas continued unabated in the last year of study. It is also evident that agricultural and forestlands have decreased in 2022 (Fig. 4).

The comparison of LULC for the years 1986, 2003 2015 and 2022 revealed that urban/built-up areas increased throughout the study period. There was a reduction in agricultural lands and a decrease in forestlands in 2003 but an increment was observed for forestlands in 2015 and a decline in the last year of the study. An upward increase in urban/built-up from an initial 5.22% (1986 – 2003) and a further upward adjustment of 8.74% (2003 – 2015) was observed. From 2015 to 2022, 8.30% of urban/built-up

areas were added. However, agricultural lands had the highest rate of decrease of – 4.37% between 1986 and 2003 and an appreciable decline of – 9.02% between 2003 and 2015. Agricultural lands decreased by 2.52% in 2022. Forestlands had a percentage change of – 1.42% between 1986 and 2003 and a marginal percentage increase of 0.71% from 2003 to 2015 and finally, decreased by 1.78% in 2022. The water environment experienced the least changes as aforementioned in the general description (Table 3).

Furthermore, the annual rate of change (*Ceteris paribus*) revealed that urban/built-up increased throughout the study period. It recorded the highest rate of change (0.92)

Table 3 Distribution of LULC

Land use land cover categories	1986		2003		2015		2022	
	Area (ha)	Area (%)	Area (ha)	Area (%)	Area (ha)	Area (%)	Area (ha)	Area (%)
Urban/Built-up	14,864.40	63.52	16,085.20	68.74	18,130.30	77.48	19,136.11	81.78
Agricultural lands	6319.08	27.00	5295.87	22.63	3184.74	13.61	2595.60	11.39
Forestlands	1288.35	5.51	955.62	4.08	1121.40	4.79	704.16	3.01
Water	928.62	3.97	1063.80	4.55	963.99	4.12	964	3.82
TOTAL(ca)	23,400.00	100.00	23,400.00	100.00	23,400.00	100.00	23,400.00	100

between 2015 and 2022. Agricultural lands decreased drastically, especially between the period (2003–2015). The highest rate of changes occurred for forestlands occurred between 1986 and 2003 whilst the water environment recorded the least changes throughout the study period (Table 4).

### 3.2 Accuracy assessment

The quality of any thematic map is determined by its accuracy. Kappa statistic was used to measure the agreement between the classified satellite images and the training samples or the reference data.

The kappa statistic using the RF classifier produced accuracies for 1986, 2003, 2015 and 2022 of 85.3%, 96.0%, 94.7% and 96.0% respectively. The producer and user and accuracies are outlined in Appendix 1.

### 3.3 Land use land cover modelling

The urban/built-up was the major transition model studied, and as a result, the vital transitions from other LULC classes were explored. Cramer's V indicated the potential explanatory strength of a driving factor in spatial urban expansion (Table 5). Cramer's V value greater than or equal to 0.15 for any driving factor was regarded as valuable, but if values are higher than or equal to 0.4, the Cramer's V value was considered very good [80]. The next procedure was to run the sub-model of important transitions, and the transition maps were generated. The LULC map of 2015 was simulated. It yielded quite satisfactory LULC predictions.

#### 3.3.1 Validation of LULC maps

Figure 5 depicted the validated projection that illustrated the accuracy accomplished by the model. The maps were composed of hits, misses, false alarms and null successes. The visualisation revealed that null success was dominant.

**Table 5** Cramer's V driving factors for the potential Land Use Land Cover Changes in 2030

Driving force	Cramer's V
Distance from roads	0.30
Distance from Urban	0.29
Elevation	0.06
Slope	0.03

The misses were observed, mostly in the validated map. However, the false alarms were less observed in the validated map but the hits were sparsely distributed.

#### 3.3.2 Projection of land use land cover into 2030

The Land Use Land Cover (LULC) projection into the year 2030. The dominant class for the projected maps was urban/built-up areas. The water environment on the western boundary maintained its shape for Accra. However, the agricultural and forestlands were mostly found in the upper boundary of Accra and gradually spread into the central portions of Accra (Fig. 6).

#### 3.3.3 Areal extent of land use land cover in 2030

The urban/built-up areas are projected to occupy 19053 ha (81.4%). Agricultural lands are tipped to cover 1897 ha (8.1%). However, forestlands are expected to have 1509 (6.5%) and 941 (4.0%) in 2030. Nevertheless, the water environment is forecasted to maintain almost its areal extent in 2030 (Table 6).

### 3.4 Spatial urban expansion analysis

To expedite the analysis of the trend of expansion of the urban/built-up areas, the pixels of urban/built-up were extracted from the classified images. The overlay of the urban/built-up areas of the selected years showed the

**Table 4** Changes in area and percentages

Land Use Land Cover Categories	1986 – 2003		2003 – 2015		2015 – 2022		Annual Rate of Change (%)		
	Area (ha)	Percentage Change (%)	Area (ha)	Percentage Change (%)	Area (ha)	Percentage Change (%)	1986–2003	2003 – 2015	2015 – 2022
Urban/Built-up	1220.80	5.22	2045.10	8.74	1505.81	6.44	0.31	0.73	0.92
Agricultural lands	– 1023.21	– 4.37	– 2111.13	– 9.02	– 589.14	– 2.52	– 0.26	– 0.75	– 0.32
Forestlands	– 332.73	– 1.42	165.78	0.71	– 417.24	– 1.78	– 0.08	0.06	– 0.25
Water	135.18	0.58	– 99.81	– 0.43	0.01	0.00	0.03	– 0.04	– 0.04

<sup>a</sup> Negative sign indicates decrement

**Fig. 5** Validated maps of 2022

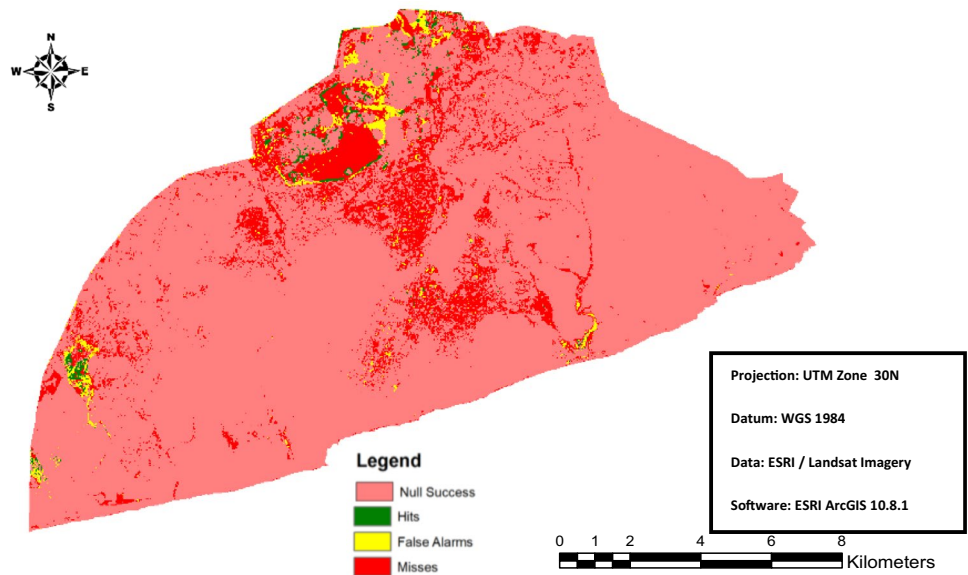


**Fig. 6** Land Use Land Cover projections into 2030

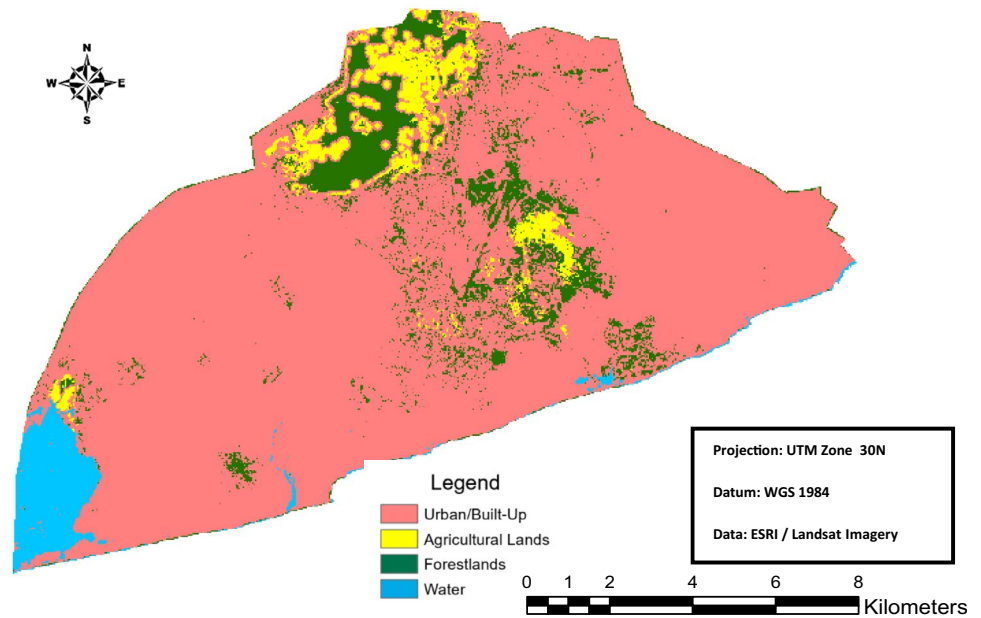


**Table 6** Area in hectares and percentages

LULC	Area (Ha)	Percentage (%)
Urban/Built-Up	19,053	81.4
Agricultural Lands	1897	8.1
Forestlands	1509	6.5
Water	941	4.0
TOTAL (ca.)	23,400.0	100.0

extent of spatial urban expansion that occurred from 1986 to 2022. Figure 7 revealed the urban/built-up areas throughout the study period.

### 3.4.1 Spatial urban expansion in the sub-metropolitan zones

The Accra Metropolis was segmented into 5 sub-metropolitan zones: Ablekuma, Ayawaso, Kpeshie, Okaikoi and Osu Klottey. The spatial urban/built-up maps were overlaid with the respective zones to depict the spatial occurrence and the area covered in each zone (Fig. 8).

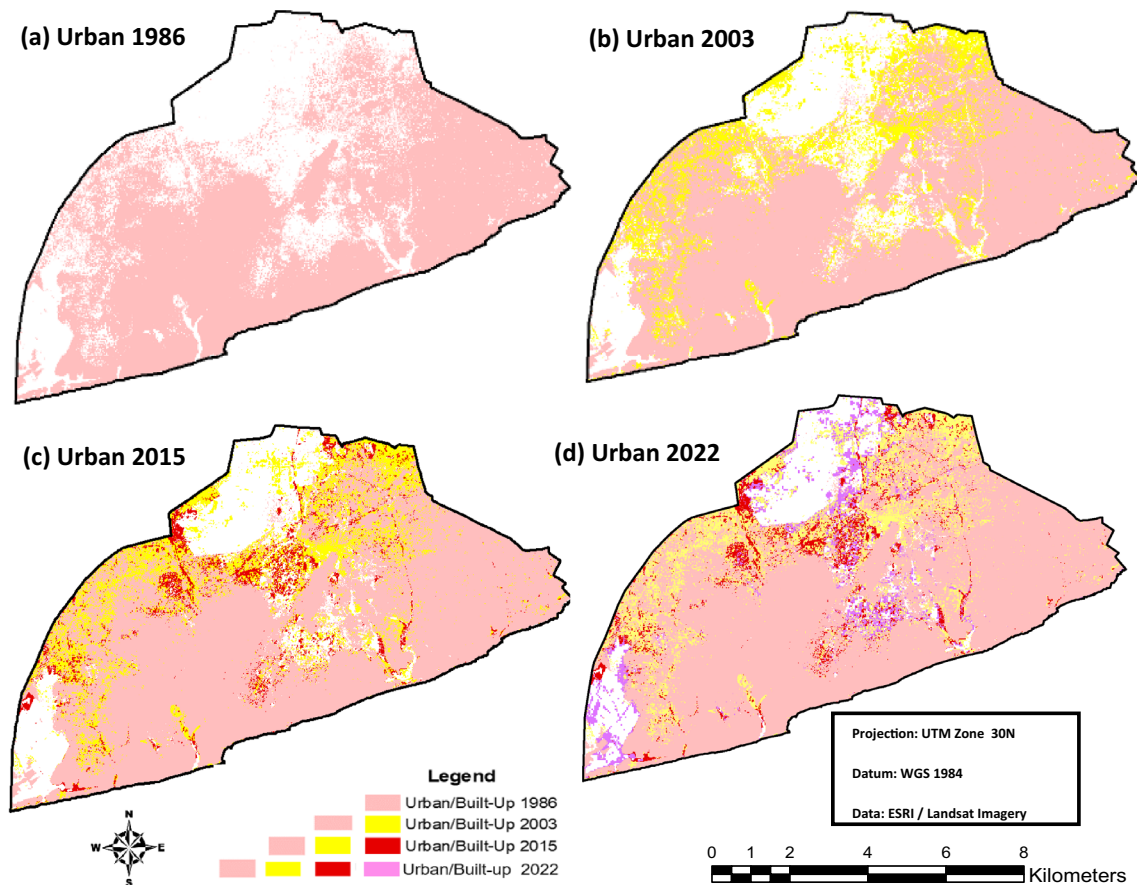


Fig. 7 Spatial urban expansion in Accra

### 3.4.2 Spatial urban extent in each sub-metropolitan area

The years 1986, 2003, 2015 and 2022 yielded urban extents of 14,707, 16,159, 16,997 and 19,497 ha respectively. Kpeshie had the highest urban extent whilst Osu Klottey had the lowest urban extent for the entire study period. In 1986, the urban extent ranged from 1524 to 6421 ha. However, in 2003, it ranged from 1242 to 6482 ha. In 2015, the values were from 1586 to 6608 ha. In 2022, the urban extent ranged from 1573 to 7308 ha. Between the years 1986 and 2003, the Ayawaso zone recorded the highest rise of 713 ha, followed by Okaikoi (366 ha), Ablekuma (293 ha), Kpeshie (61 ha) and finally Osu Klottey (18 ha). Interestingly, between 2003 and 2015, the zones ranked the same way as between 1986 and 2003 except for variations in values (Table 7).

### 3.4.3 Urban expansion analysis along a major road

The highway used was the George Walker Bush Highway with a road stretch of 35 km. The expansion was mainly found in the southern parts of the created buffers. The

significant area in the northern parts of the study area were mainly forestlands (Fig. 9).

### 3.4.4 Density of spatial urban expansion

The total area covered by urban/built-up areas ranged from 1253 to 8542 from the 500 m to 4000 m buffer. The total area was from 1388 ha to 14,499 ha. There was a decreasing trend in the density of spatial urban expansion from the 500 m to the 4000 m buffer as the values ranged from 0.90 to 0.59 (Table 8).

### 3.4.5 Density decay curve

The relationship between the distance to a major road and the density of urban expansion showed a decreasing trend. The linear regression also indicated an inverse relationship between the two sets of variables (Fig. 10).

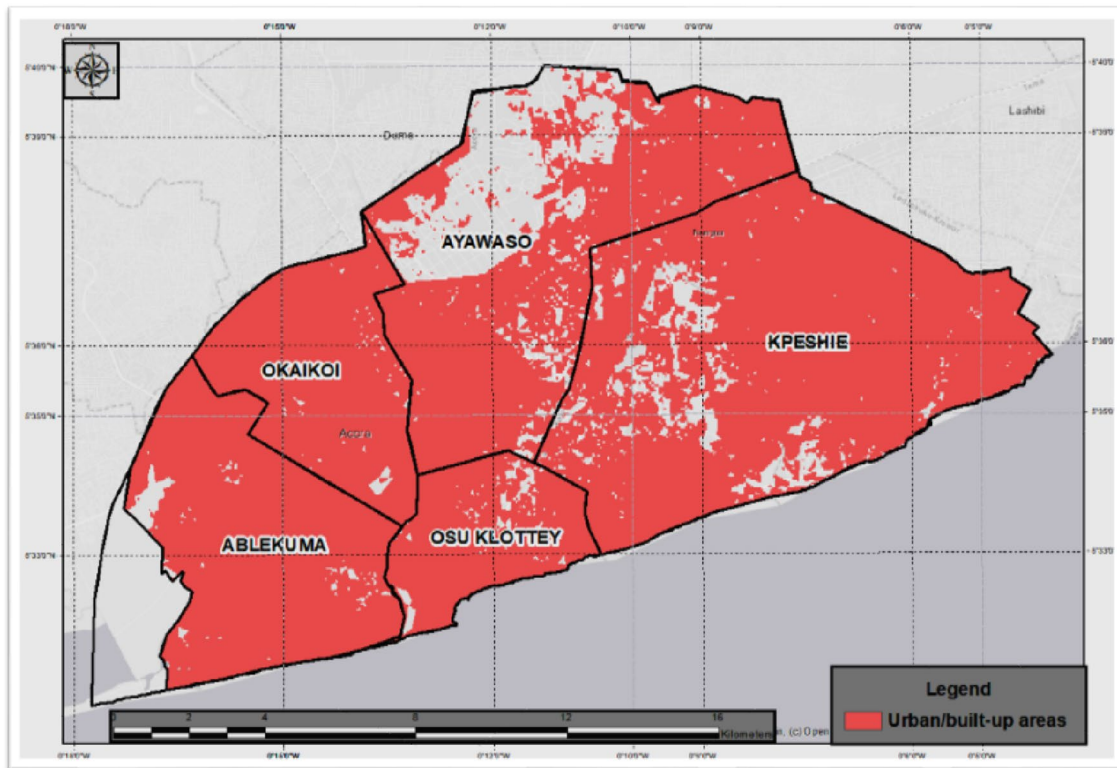


Fig. 8 Spatial urban/built-up areas in the sub-metropolitan area

Table 7 Urban Extent in each sub-metropolitan in Accra

Sub-Metro-politan	1986		2003		2015		2022	
	Urban Extent (ha)	Urban Extent (%)	Urban Extent (ha)	Urban Extent (%)	Urban Extent (ha)	Urban Extent (%)	Urban Extent (ha)	Urban Extent (%)
Ablekuma	2843	19	3136	19	3252	19	3673	20
Ayawaso	2090	14	2803	17	3120	18	4377	22
Kpeshie	6421	44	6482	40	6608	39	7308	37
Okaikoi	1830	13	2196	14	2432	14	2566	13
Osu Klottey	1524	10	1542	10	1586	10	1573	8
Total (ca)	14,708.0	100.0	16,159.0	100.0	16,998.0	100.0	19,497.0	100.0

### 3.5 Remote sensing indices

#### 3.5.1 General overview of NDVI

The NDVI values ranged from -0.38 to 0.54. Matching the NDVI and LULC maps of Accra (Fig. 2), the visual interpretation broadly indicated that the lowest values for NDVI were recorded in the water environment located on the western boundary of Accra. It was observed that the urban/built-up areas produced low values for NDVI, followed by agricultural lands. Visually, the highest values were recorded in the forestlands. The above pattern was uniform for the NDVI maps of 1986, 2003, 2015 and 2022 (Fig. 11).

#### 3.5.2 General overview of NDBI

The NDBI values ranged from - 0.25 to 0.43. The visualisation revealed that the lowest values were recorded in the water environment followed by the agricultural and forestlands in the NDBI maps. The portions classified as urban/built-up yielded the highest values for NDBI. The 2003 imagery produced similar patterns as the 1986 satellite imagery. The 2015 and 2022 NDBI maps had the forestlands also record lower values in the water environment whilst the agricultural lands produced moderate values and ultimately, urban/built-up recorded the highest values for NDBI (Fig. 12).

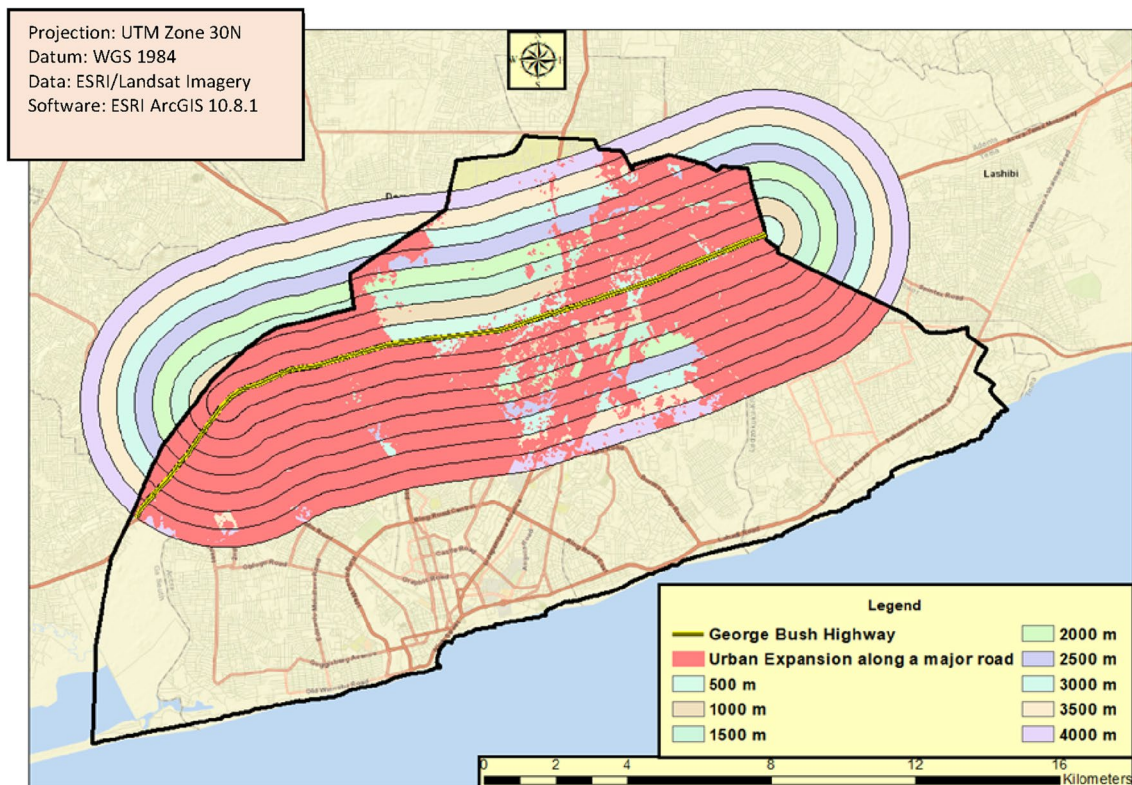


Fig. 9 Urban extent in 500 m buffer along a major road

Table 8 Density of spatial urban expansion

Buffer	Area	Total area	Density of spatial urban expansion
500 m	1253	1388	0.90
1000 m	2518	2877	0.88
1500 m	3631	4494	0.81
2000 m	4703	6239	0.75
2500 m	5737	8110	0.71
3000 m	6752	10,112	0.67
3500 m	7625	12,241	0.62
4000 m	8542	14,499	0.59

### 3.6 Retrieval of land surface temperature

The daily temperature values ranged from 19.3 to 33.3 °C. It was noticed that temperature values for 1986 were the least compared to the other study years. It was also observed that the water component and the forestlands produced very low temperatures. Visually, the urban/built-up areas produced higher temperatures in comparison to the other LULC types. The agricultural lands produced moderate temperatures throughout the study period (Fig. 13).

### 3.7 Correlation analyses

It was observed that the coefficients showing the relationships between LST and NDBI were higher than between LST and NDVI. There was a negative correlation between NDVI and LST, likewise NDVI and NDBI throughout the entire study period. However, a higher positive correlation was observed between NDBI and LST (Table 9).

### 3.8 Comparison of OLS and GWR

Comparing model diagnostics was considered one of the best ways to assess the performance of models and thus, OLS and GWR were compared using their adjusted R squared and AICc values.

Generally, GWR yielded higher values for the adjusted R squared compared to OLS. Similarly, it also produced smaller values for AICc when ranked with the OLS. It was therefore evident that the GWR models performed better than the OLS models (Table 10).

The coefficient for the three years was positive as observed from the equations. Although both coefficients produced positive numbers, the coefficients of NDBI produced higher values compared to NDVI.

**Fig. 10** Density Decay Curve of Accra

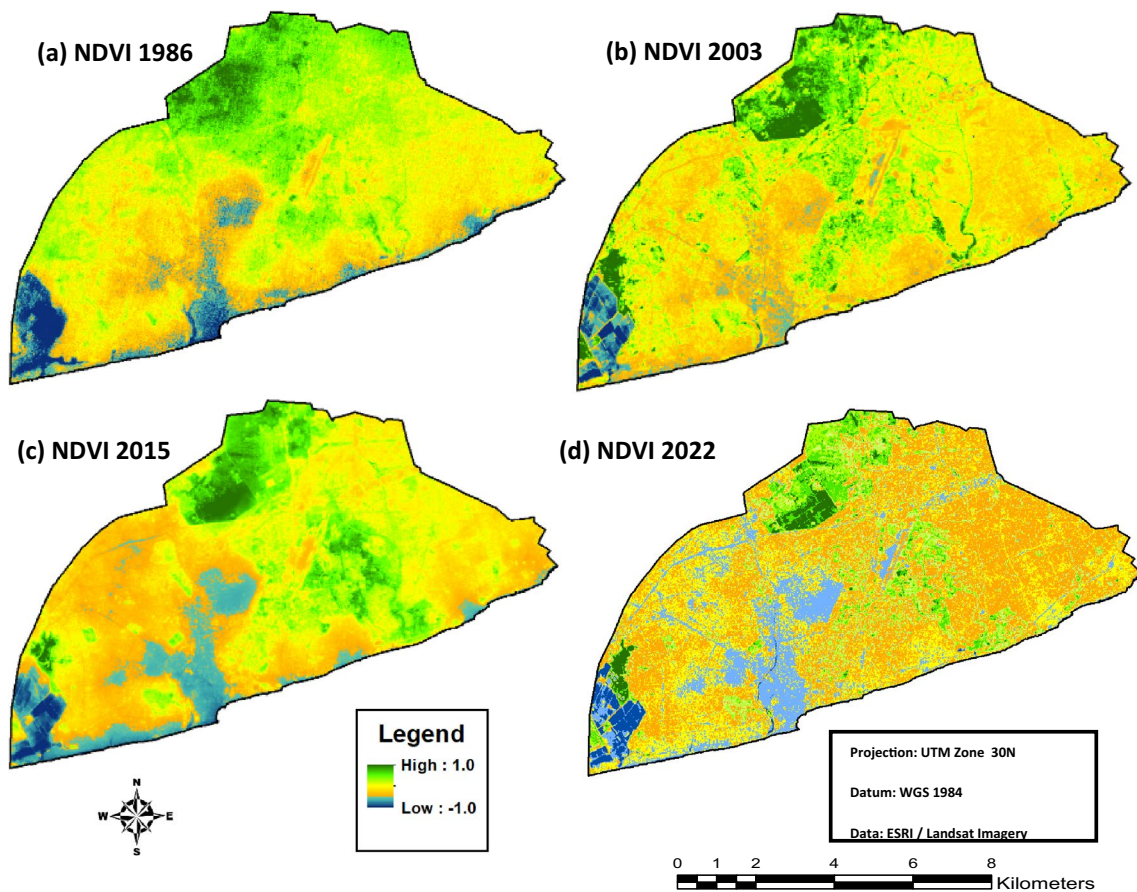
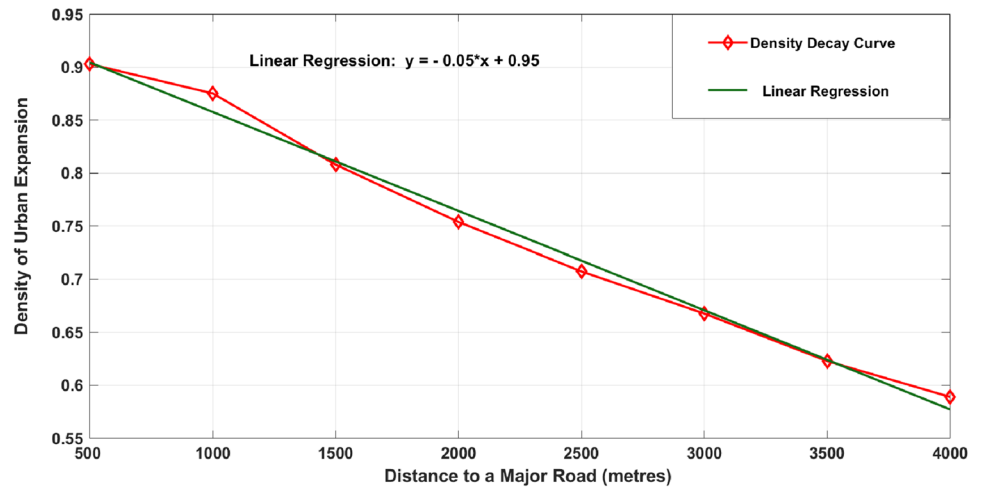


**Fig. 11** General overview of Normalised Difference Vegetation Index

The following equations were derived to showcase the relationship between the dependent variable (LST) and the independent variables (NDVI and NDBI).

The equation for the satellite image for 1986 was;

$$LST = 21.39 + (-5.57 * NDVI) + (12.15 * NDBI) + E \tag{11}$$

The equation for the satellite image for 2003 was;

$$LST = 27.22 + (-1.17 * NDVI) + (8.34 * NDBI) + E \tag{12}$$

However, the equation for the satellite image for 2015 was;

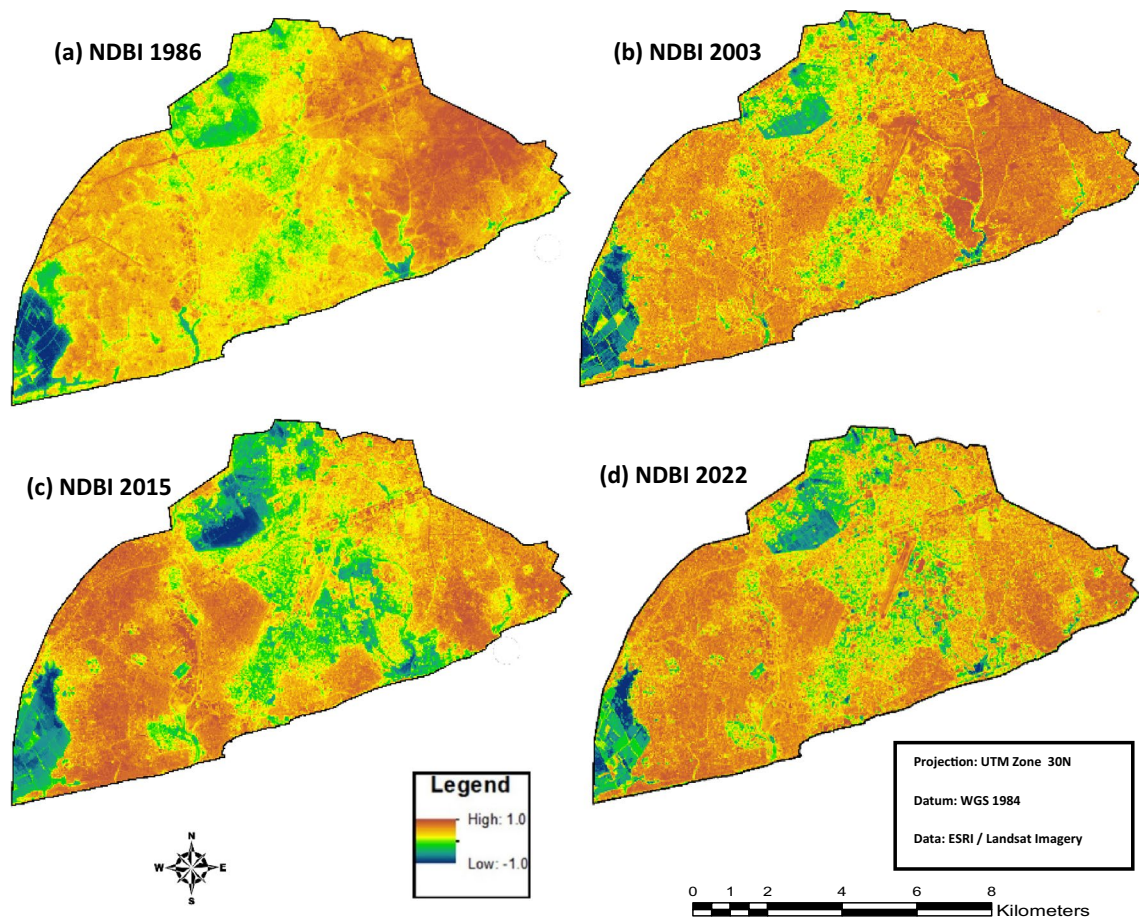


Fig. 12 General overview of Normalised Difference Built-up Index in Accra

$$LST = 27.59 + (-8.39 * NDVI) + (21.09 * NDBI) + E \tag{13}$$

Finally, the equation for the satellite image of 2022 was;

$$LST = 28.95 + (-9.42 * NDVI) + (24.05 * NDBI) + E \tag{14}$$

where E is the error term.

## 4 Discussion

### 4.1 Classification of satellite imageries and their assessed accuracy

The random forest classification algorithm utilised the pixel values to delineate the different Land Use Land Cover types. The evaluation criteria for the classified satellite images were based on their classification accuracies. The kappa statistics of the classified LULC maps were above 85% regarded as the minimum standard set by the USGS classification scheme [65]. The user and

producer accuracies and kappa statistics produced excellent results. These results were compared to the work of [61] that used RF classification. The kappa statistics obtained in the works of [16, 25, 60, 81] in Ghana using the Maximum Likelihood Classifier were lower compared to the results obtained using the RF classifier in this research. The initial works of [82, 83] revealed the superiority of the RF classifier over other types of classification algorithms. The extraction of the different LULC types using Landsat satellite imagery provided insights that sought to contribute to the existing knowledge on the usage of random forest algorithm for satellite image classification. Therefore, it upgraded the traditional extraction techniques classifiers utilised in satellite image classification in Accra and other study areas in Ghana. Therefore, attention should be shifted to the utilisation of machine learning algorithms for the classification of LULC classes by researchers, especially in Ghana.



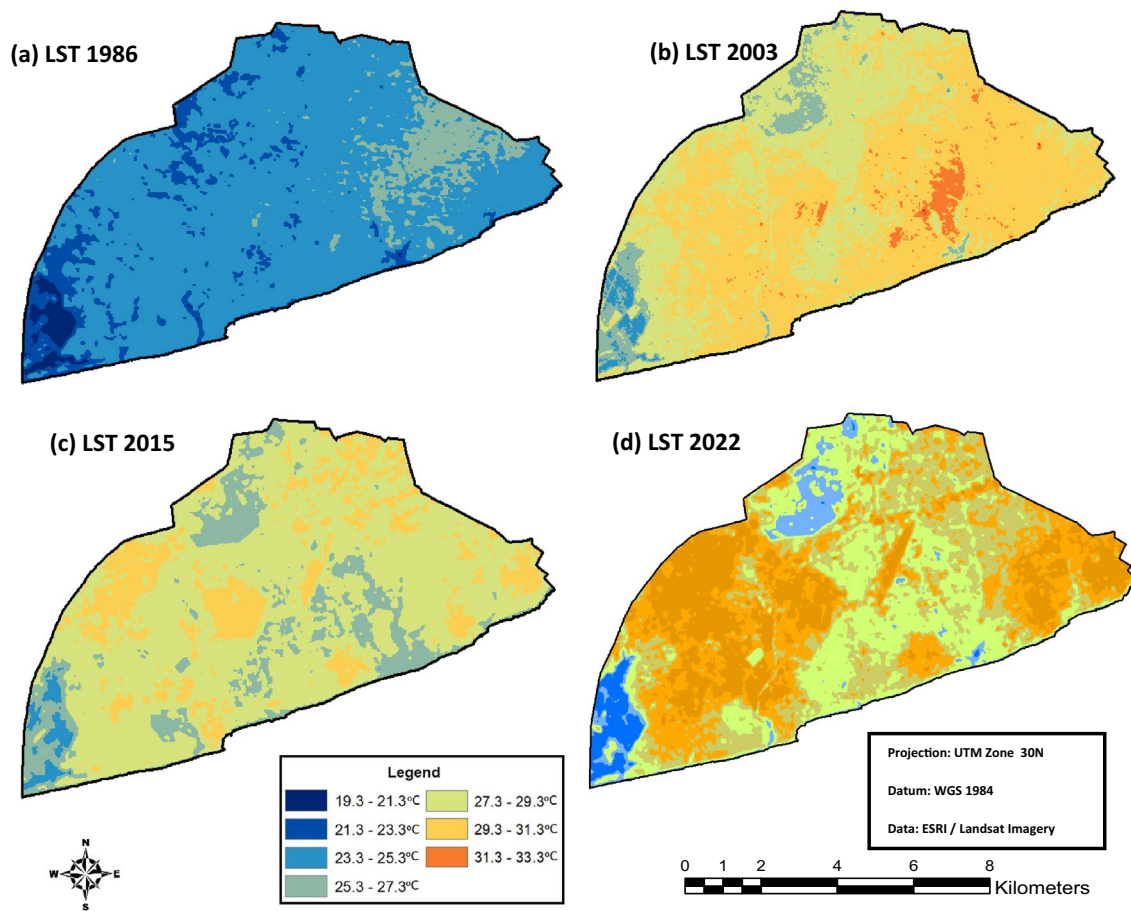


Fig. 13 General overview of land surface temperature

Table 9 Correlation analysis amongst the RS indices

RS indices	LST				NDVI			
	1986	2003	2015	2022	1986	2003	2015	2022
NDVI	-0.57	-0.72	-0.91	-0.93				
NDBI	0.83	0.75	0.90	0.92	-0.59	-0.94	-0.95	-0.97

Table 10 Evaluation of OLS and GWR based on model diagnostics

Parameter	LST 1986		LST 2003		LST 2015		LST 2022	
	OLS	GWR	OLS	GWR	OLS	GWR	OLS	GWR
Adjusted R <sup>2</sup>	0.70	0.94	0.64	0.93	0.67	0.96	0.72	0.95
AICc	459,439	16,645	592,856	174,780	490,145	8167	610,422	9564

### 4.2 Land use land cover

Spatial urban expansion began along the coast of Accra before 1986 and spread upwards and outwards to the other areas of Accra as observed from the classified images. The LULC maps revealed that most urban/built-up areas were close to the coastline (southern boundary of the Metropolis) in Accra. The depletion of agricultural lands

in the classified image of 2003 could be attributed to the increased demand for land for residential and commercial hubs. The reduction in the forestlands may have resulted from the illegal logging of trees in Accra. This assertion supports the earlier works of [84, 85] that concluded that forestlands were depleted in the Metropolis. The classified image of 2015 also revealed a higher proportion of urban/built-up areas with agricultural lands decreasing.

The visual inspection indicated a rise in forestlands and it might be attributed to the afforestation activities and stringent measures put in place by the Forestry Commission of Ghana through its afforestation programmes [86]. The water environment visually appeared to have maintained its shape throughout the study.

The analysis of the LULC maps revealed a continuous increase in the urban/built-up areas at the expense of agricultural and forestlands. The increase in population is a distinct factor that could have triggered spatial urban expansion in supporting the outcome of the works of [26, 87, 88]. The increased nexus between urban/built-up areas and population could be attributed to the architectural style of buildings that are dominated by the horizontal spread of houses (one-storey houses) without making use of vertical space (two or more storey buildings) [89, 90]. In Ghanaian society, house ownership apart from the provision of shelter serves as a higher indicator of one's social status and prominence in society [91]. Moreover, for most Ghanaians, the ownership of lands and houses is key and necessary for attaining pride which is an integral part of their traditions and culture [92]. Therefore, spatial urban expansion could be due to the uncontrolled individual usage of land as most people prefer to buy lands at the urban fringes where lands for development into urban/built-up areas have relatively lower prices [93].

The results indicate that the focus has been on the transformation of different LULC into urban/built-up areas. The scramble for land for the construction of housing units could lead to the continuous transformation of other LULC types into urban/built-up areas. It might also increase the conflict among the populace over the ownership of lands. It is urged that the lands commission of Ghana, traditional authorities and communities and the Ministry of Works and Housing may have to collaborate to control the accelerated spatial urban expansion through education and enforcement of the policies related to land use in Accra and other developing cities in Ghana.

### 4.3 Spatial urban expansion

Accra's spatial urban expansion trend was found to be outwards and northwards. Demand for residential land may be the primary cause of spatial metropolitan growth. According to the findings of the study, urban/built-up areas have been under intense pressure [17, 27, 94]. It was recorded that 50% of the structures in the Metropolis were single-story compound houses, with the majority of multi-story buildings not exceeding the third floor [95, 96].

Osu Klottey had the least geographic urban growth among Accra's sub-metropolitan zones. This could be ascribed to the fact that the first Accra settlers resided in Osu Klottey, leaving smaller sections for future spatial urban growth. The presence of most governmental organisations

in Osu Klottey during the colonial and post-independence periods could be ascribed to spatial urban growth [97]. The spatial urban growth was most noticeable in the northern sections of the Ablekuma, Okaikoi, and Kpeshie sub-metropolitan zones, which were heavily transformed from other LULC types to urban/built-up areas. The spatial urban expansion revealed in this study backs up the findings of [98], who found that Accra witnessed earlier spatial urban expansion.

The declining tendency in the density decay curve supported the previous work of [99, 100] that Accra had been growing before the 1980s. Some of the noted effects of spatial urban growth included intrusion on farming and forestlands for domestic and business purposes. Public open spaces, particularly green spaces, have been converted into urban/built-up regions [101].

The distance to a main road had a negative association with the density of spatial urban growth. For places further away from the George Bush Highway, the population decreased. The distance to a main route had a negative association with the density of spatial urban growth. The greater the distance from the George Bush Highway, the lower the intensity of spatial metropolitan growth. The closeness of social facilities to the highway may explain the trend. City planners prefer to build near highways to take benefit of established facilities and social amenities. As the extent of the buffer grew, non-urban regions were converted into urban/built-up areas.

This suggests that the scramble for land near a major highway appears to be unabated. Other types of flora and fauna may be impacted, emphasising their numbers and ecological significance to the ecosystem's equilibrium. The impacts of these conversions are not examined with a primary emphasis on the growth of the lands for business or residential uses.

### 4.4 Analysis of Remote Sensing Indices (NDVI, NDBI) and LST

The general overview of NDVI and NDBI revealed that urban/built-up areas produced lower values for NDVI but higher values for NDBI. This situation is the reverse for both agricultural areas and forestlands. In the case of the water environment, it recorded the lowest values for both NDVI and NDBI. This outcome was similar to the works of [38, 102] in Abuja (Nigeria); Florence and Naples (Italy) respectively.

The highest temperature values were recorded in the urban/built-up areas because these areas store more solar energy, as was also observed by (Adeyeri et al., 2017). Agricultural and forestlands reflect a moderate amount of solar radiation and play a vital role in the modification of land surface temperature (Adeyeri et al., 2017; Li et al., 2016). Therefore, it was expected that the temperature around the south-western boundary of Accra covered by water

produced the least temperature for the city-level evaluation of LST due to a higher reflection of radiation [38, 40, 42, 105]. Temperature values in 1986 were the least whilst the highest values were recorded in 2022. However, LST in 2003 was higher than in 2015. This was quite surprising and could be attributed to the different months during which the satellite images of 2003 and 2015 were taken. The satellite images of 1986 2015 and 2022 were taken in December, whilst that of 2003 was taken in February.

The results imply that there could be ineffective and inefficient ways of buffering environmental temperature throughout the study period. The reduction of the agricultural and forestlands without proper planning to incorporate the various LULC types may have generally led to decreased green areas (agricultural and forestlands) as NDVI decreased throughout the study. It is therefore important for city planners to incorporate practical environmental sustainability policies. When these policies are not implemented, there could be an increase in land surface temperature which might affect human lives and other living organisms in the environment.

#### 4.5 Correlation analysis

The correlation analysis also revealed similar patterns as the relationships between LST and NDBI, which was positive. This outcome is comparable to the works of [106, 107]. The relationship may be described as stronger. However, the correlation between LST and NDVI was negative. Similar correlation patterns were revealed in the works of [102, 108] and illustrated that NDVI has a negative correlation with LST. The correlation between NDVI and NDBI was negative throughout the study years and could be described as strong. This is also similar to earlier works [40, 109].

Therefore, it is imperative to protect the forestlands, especially the Achimota forest in Accra, by the Forest Commission as further encroachment into the forest reserve in Accra could further increase and decrease the correlation between LST/NDBI and LST/NDVI, respectively. This could have adverse effects on the balance of the provision of ecosystem services.

#### 4.6 Ordinary least squares and geographical weighted regression

The relationship between LST and (NDBI/NDVI) was assessed. The outcome of OLS regression revealed a significant positive correlation between LST and NDBI, whilst a significant negative correlation was revealed between LST and NDVI. This outcome agreed with the negative linear relationship between mean LST and NDVI values in the works of [45, 110–112]. The variable NDBI had a larger influence on LST prediction based

on the equations for OLS regression. This corroborated with the findings of [45, 47] that concluded that the most influential biophysical parameter of LST variation was NDBI. The inland water environment of Accra yielded a negative correlation between LST and NDVI and was comparable to the findings of the work of [46]. This outcome was in line with the findings related to the UHI effect, in Quanzhou City [113] and some megacities of Southeast Asia [114]. These initial works indicated a significant positive correlation between mean LST and the density of impervious surfaces, whilst this correlation was negative for green areas [115].

It can be argued that the GWR model's prediction accuracy was better than OLS as the works of [50, 102] revealed similar results compared to this work. It was found that GWR performed better, and it is attributed to the fact that there was the inclusion of the spatial component as emphasised in the research of [116].

The findings from the regression analysis between LST and (NDVI/NDBI) will serve as a base study for further research by the scientific community, especially for related studies in Ghana and other tropical countries. The regression analysis also revealed that more attention had been given to the spatial urban expansion of urban/built-up areas without consideration for green areas (agricultural and forestlands). This could lead to exposure to high radiation from the sun, which may not be well for the general well-being of humans and other mammals in urban/built-up areas.

## 5 Conclusions

The Accra Metropolis was used as the test site to address the relationship between spatial urban expansion on temperature by integrating RS, temperature observations and GIS modelling approaches. The limited cloud-free Landsat series of sensors (TM, ETM, and OLI) and temperature observations were mainly employed for this research. The LULC classification scheme grouped the study area into urban/built-up areas, agricultural, forestlands and the water environment. The classified images of all the study areas revealed that urban/built-up areas dominated the other LULC classes throughout the timeframe of the study.

The techniques used in tracking spatial urban expansion (i.e. spatial urban expansion in sub-metropolitan zones, buffer (500 m), density of spatial urban expansion (density decay curve, correlation between density of spatial urban expansion and distance from a major road) revealed that there was an imbalance for lands for spatial urban expansion (housing units, infrastructural projects, and economic activities) on one side and the preservation of forested areas on the other).

Another vital part of this research was on the intense impervious surfaces occurring that have increased urban

temperature. The relationship was addressed in this research to ascertain the alterations in temperature and urban expansion effects on temperature. The satellite images were employed to retrieve the RS indices and Land Surface Temperature. The RS indices and the statistical approaches were useful for the assessment of the spatiotemporal distribution of temperature. The OLS Regression and the GWR yielded satisfactory results in modelling LST with (NDBI and NDVI). It was found that the urban/ built-up areas accelerated temperature and that is in sharp contrast with agricultural, forestlands and the water environment that decreased temperature regarding the developed equations (11–13). The study proved beneficial for the investigation of the adverse effects of urban expansion on the local temperature.

The interplay of the RS indices revealed rudimentary relationships among them. The correlation analysis between the extracted land surface temperature and NDVI revealed a negative correlation and a positive relationship between LST and NDBI. It aided in showcasing the roles LULC changes most notably urban expansion plays in the alteration of the urban temperature.

Decision-makers can utilise this information to evaluate the effectiveness of existing land use policies and regulations in managing urbanisation impacts on temperature. It can help identify areas where land use practices have contributed to temperature increases and guide the development of targeted interventions to promote sustainable land use planning and design. The findings of this research may guide the implementation of green infrastructure, urban greening initiatives, and the promotion of climate-responsive urban design to enhance thermal comfort, reduce energy consumption, and improve overall liveability.

This study, therefore, concludes that there is a causal relationship between spatial urban expansion and temperature. The limitation of this study included the inability to obtain very high-resolution satellites for the study period. Again, the same interval of years for the study was not possible. It is recommended that Ghana should be decentralised to decrease the influx of people into Accra and also forestlands should be protected in the metropolis. It is therefore imperative that policymakers and land use planners in the Accra Metropolis should encourage urban forestry.

Future scientific investigations could enhance their findings by delving into additional factors with the potential to exert an influence on urban climate, population density and the implementation of land use policies. Moreover, subsequent works may be directed towards examining the ecological and social ramifications associated with land use transformations, aiming to identify effective strategies for ameliorating the adverse effects stemming from urbanisation. Such studies may prioritise the mitigation of the adverse consequences of spatial urban expansion on temperature. Future guidelines may

include the development of an environmental monitoring protocol that could be monthly, seasonal or yearly utilising multispectral or hyperspectral satellite images.

The integration of RS and GIS provided this research with gainful insights into spatiotemporal patterns resulting from urbanisation. It was an efficient technique used in tracking urban expansion and accessing its relationship with temperature using Landsat satellite imageries.

**Acknowledgements** The authors thank the USGS for the cost-free satellite images of Accra. We are grateful to the EuroAqua family in Cottbus and the staff at the Department of Hydrology—Brandenburg University of Technology, Cottbus—Senftenberg for their diverse support.

**Author Contributions** Conceptualisation, BFF; methodology, BFF and OFS; software, BFF; validation, BFF, AK and OFS; formal analysis, BFF; investigation, BFF; resources, BFF; data curation, BFF; writing—original draft preparation, BFF; writing—review and editing, BFF, AK and OFS; visualisation, BFF; supervision, BFF, AK and OFS; project administration, BFF. All authors have read and agreed to the published version of the manuscript.

**Funding** Open Access funding enabled and organised by Projekt DEAL. B.F.F. is grateful to the Katholischer Akademischer Ausländer—Dienst (KAAD) for the scholarship support for his PhD that gave birth to this research. Open Access publication was sponsored by Brandenburg University of Technology, Cottbus—Senftenberg.

**Data Availability** Derived data supporting the findings of this research is available from the corresponding author (BFF) on request.

## Declarations

**Conflict of interest** The authors have no competing interests to declare that are relevant to the content of this article.

**Informed Consent** Not applicable.

**Open Access** This article is licensed under a Creative Commons Attribution 4.0 International License, which permits use, sharing, adaptation, distribution and reproduction in any medium or format, as long as you give appropriate credit to the original author(s) and the source, provide a link to the Creative Commons licence, and indicate if changes were made. The images or other third party material in this article are included in the article's Creative Commons licence, unless indicated otherwise in a credit line to the material. If material is not included in the article's Creative Commons licence and your intended use is not permitted by statutory regulation or exceeds the permitted use, you will need to obtain permission directly from the copyright holder. To view a copy of this licence, visit <http://creativecommons.org/licenses/by/4.0/>.

## Appendix A

User and producer accuracies for the classified satellite images.

See Tables 11, 12, 13, and 14.

**Table 11** User, Producer and Kappa statistics for the classified image of 1986

LULC	Urban/ built-up	Agricul- tural lands	Forestlands	Water	Total	User Accuracy	Kappa
Urban/built-up	47	3	0	0	50	0.94	0
Agricultural lands	5	44	1	0	50	0.88	0
Forestlands	1	11	38	0	50	0.76	0
Water	0	0	0	50	50	1	0
Total	53	58	39	50	200	0	0
<i>Producer Accuracy</i>	0.89	0.76	0.97	1	0	0.90	0
<i>Kappa</i>	0	0	0	0	0	0	0.86

**Table 12** User, Producer and Kappa statistics for the classified image of 2003

LULC	Urban/ built-up	Agricul- tural lands	Forestlands	Water	Total	User Accuracy	Kappa
Urban/ built-up	49	1	0	0	50	0.98	0
Agricultural lands	2	47	1	0	50	0.94	0
Forestlands	0	1	49	0	50	0.98	0
Water	0	0	0	50	50	1	0
Total	51	49	50	50	200	0	0
<i>Producer Accuracy</i>	0.96	0.96	0.98	1	0	0.98	0
<i>Kappa</i>	0	0	0	0	0	0	0.97

**Table 13** User, producer and Kappa statistics for the classified image of 2015

LULC	Urban/ built-up	Agricul- tural lands	Forestlands	Water	Total	User Accuracy	Kappa
Urban/ built-up	49	1	0	0	50	0.98	0
Agricultural lands	3	46	0	1	50	0.92	0
Forestlands	0	3	47	0	50	0.94	0
Water	1	0	0	49	50	0.98	0
Total	53	50	47	50	200	0	0
<i>Producer Accuracy</i>	0.92	0.92	1	0.98	0	0.96	0
<i>Kappa</i>	0	0	0	0	0	0	0.94

**Table 14** User, producer and Kappa statistics for the classified image of 2022

LULC	Urban/ built-up	Agricul- tural lands	Forestlands	Water	Total	User Accuracy	Kappa
Urban/ built-up	49	1	0	0	50	0.98	0
Agricultural lands	2	47	0	1	50	0.94	0
Forestlands	0	2	48	0	50	0.96	0
Water	1	0	0	49	50	0.98	0
Total	53	50	47	50	200	0	0
<i>Producer Accuracy</i>	0.92	0.92	1	0.98	0	0.97	0
<i>Kappa</i>	0	0	0	0	0	0	0.96

## References

1. UNDESA (2019) World population prospects 2019, no. 141
2. Argüeso D, Evans JP, Fita L, Bormann KJ (2014) Temperature response to future urbanization and climate change. *Clim Dyn* 42(7–8):2183–2199. <https://doi.org/10.1007/s00382-013-1789-6>
3. Patino JE, Duque JC (2013) A review of regional science applications of satellite remote sensing in urban settings. *Comput Environ Urban Syst* 37(1):1–17. <https://doi.org/10.1016/j.compevnurbsys.2012.06.003>
4. UNDESA (2018) World urbanization prospects, vol 12. UNDESA, New York
5. Duranton G (2015) Growing through cities in developing countries. *World Bank Res Obs* 30(1):39–73. <https://doi.org/10.1093/wbro/lku006>
6. Cobbinah PB, Erdiaw-Kwasie MO, Amoateng P (2015) Africa's urbanisation: Implications for sustainable development. *Cities* 47:62–72. <https://doi.org/10.1016/j.cities.2015.03.013>
7. Cohen B (2006) Urbanization in developing countries: current trends, future projections, and key challenges for sustainability. *Technol Soc* 28(1–2):63–80. <https://doi.org/10.1016/j.techsoc.2005.10.005>
8. Parnell S, Walawege R (2011) Sub-Saharan African urbanisation and global environmental change. *Glob Environ Chang* 21(SUPPL. 1):S12–S20. <https://doi.org/10.1016/j.gloenvcha.2011.09.014>
9. Ghana Statistical Service (GSS) (2014) Accra Metropolitan. <https://new-ndpc-static1.s3.amazonaws.com/CACHES/PUBLICATIONS/2016/06/06/AMA.pdf>
10. Ghana Statistical Service (GSS) (2021) Population of regions and districts
11. Ministry of Lands and Forestry, "National Land Policy," 1999.
12. R. A. Acheampong, Local-level spatial planning and development management. 2019.
13. Songsore J (2003) Towards a better understanding of urban change: urbanization. National Development and Inequality in Ghana. Ghana Universities Press, Ghana
14. Seto KC, Güneralp B, Hutyra LR (2012) Global forecasts of urban expansion to 2030 and direct impacts on biodiversity and carbon pools. *Proc Natl Acad Sci USA* 109(40):16083–16088. <https://doi.org/10.1073/pnas.1211658109>
15. Turrini T, Knop E (2015) A landscape ecology approach identifies important drivers of urban biodiversity. *Glob Chang Biol* 21(4):1652–1667. <https://doi.org/10.1111/gcb.12825>
16. Yeboah F, Awotwi A, Forkuo EK, Kumi M (2017) Assessing land use and land cover changes due to urban growth in Accra. *J Basic Appl Res Int* 22(2):43–50
17. Wemegah CS, Yamba EI, Aryee JNA, Sam F, Amekudzi LK (2020) Assessment of urban heat island warming in the greater accra region. *Sci. African* 8:426. <https://doi.org/10.1016/j.sciaf.2020.e00426>
18. Abass K, Adanu SK, Gyasi RM (2018) Urban sprawl and land use/land-cover transition probabilities in peri-urban Kumasi, Ghana. *West Afri J Appl Ecol* 26:118–132
19. C. D. Elvidge, F. C. Hsu, K. E. Baugh, and T. Ghosh, National trends in satellite-observed lighting 1992–2012. 2014.
20. Mertes CM, Schneider A, Sulla-Menashe D, Tatem AJ, Tan B (2015) Detecting change in urban areas at continental scales with MODIS data. *Remote Sens Environ* 158:331–347. <https://doi.org/10.1016/j.rse.2014.09.023>
21. Fenta AA et al (2017) The dynamics of urban expansion and land use/land cover changes using remote sensing and spatial metrics: The case of Mekelle city of northern Ethiopia. *Int J Remote Sens* 38(14):4107–4129. <https://doi.org/10.1080/01431161.2017.1317936>
22. Frimpong BF, Molkenhain F (2021) Tracking urban expansion using random forests for the classification of landsat imagery (1986–2015) and predicting urban / built-up areas for 2025 : a study of the Kumasi Metropolis, Ghana, vol 10, no. 44. <https://doi.org/10.3390/land10010044>.
23. Tempfli et al K (2013) AGERE! 2013—Proceedings of the 2013 ACM Workshop on Programming Based on Actors, Agents, and Decentralized Control. In: AGERE! 2013—Proc. 2013 ACM Work. Program. Based Actors, Agents, Decentralized Control
24. J. R. Jensen, Introductory Digital Image Processing, vol. 4, no. 3. 2015.
25. Attua EM, Fisher JB (2011) Historical and future land-cover change in a municipality of Ghana. *Earth Interact* 15(9):1–26. <https://doi.org/10.1175/2010EI304.1>
26. Addae B, Oppelt N (2019) Land-Use/Land-Cover Change Analysis and Urban Growth Modelling in the Greater Accra Metropolitan Area (GAMA), Ghana. *Urban Sci* 3(1):26. <https://doi.org/10.3390/urbansci3010026>
27. Buo I, Sagris V, Burdun I, Uuemaa E (2020) Estimating the expansion of urban areas and urban heat islands (UHI) in Ghana: a case study. *Nat Hazards*. <https://doi.org/10.1007/s11069-020-04355-4>
28. B. F. Frimpong, "Land Use and Cover Changes in the Mampong Municipality of the Ashanti Region," Kwame Nkrumah University of Science and Technology, 2015.
29. Frimpong BF, Koranteng A, Molkenhain F (2022) Analysis of temperature variability utilising Mann-Kendall and Sen's slope estimator tests in the Accra and Kumasi Metropolises in Ghana. *Environ Syst Res* 11(1):1–13. <https://doi.org/10.1186/s40068-022-00269-1>
30. Subedi P, Subedi K, Thapa B (2013) Application of a hybrid cellular automaton-Markov (CA-Markov) model in land-use change prediction: a case study of Saddle Creek Drainage Basin, Florida. *Appl Ecol Environ Sci* 1(6):126–132. <https://doi.org/10.12691/aees-1-6-5>
31. Han H, Yang C, Song J (2015) Scenario simulation and the prediction of land use and land cover change in Beijing, China. *Sustainability* 7(4):4260–4279. <https://doi.org/10.3390/su7044260>
32. Hegazy IR, Kaloop MR (2015) Monitoring urban growth and land use change detection with GIS and remote sensing techniques in Daqahlia governorate Egypt. *Int J Sustain Built Environ* 4(1):117–124. <https://doi.org/10.1016/j.ijsbe.2015.02.005>
33. Mahmoud MI, Duker A, Conrad C, Thiel M, Ahmad HS (2016) Analysis of settlement expansion and urban growth modelling using geoinformation for assessing potential impacts of urbanization on climate in Abuja City, Nigeria. *Remote Sens*. <https://doi.org/10.3390/rs8030220>
34. Anand V, Oinam B (2020) Future land use land cover prediction with special emphasis on urbanization and wetlands. *Remote Sens Lett* 11(3):225–234. <https://doi.org/10.1080/2150704X.2019.1704304>
35. Saputra MH, Lee HS (2019) Prediction of land use and land cover changes for North Sumatra, Indonesia, using an artificial-neural-network-based cellular automaton. *Sustain* 11(11):1–16. <https://doi.org/10.3390/su11113024>
36. Nurwanda A, Honjo T (2020) The prediction of city expansion and land surface temperature in Bogor City, Indonesia. *Sustain Cities Soc* 52(2018):101772. <https://doi.org/10.1016/j.scs.2019.101772>
37. Koranteng A, Adu-poku I, Frimpong BF, Asamoah JN, Agyei J (2023) Urbanization and other land use land cover change assessment in the Greater Kumasi Area of Ghana, pp 363–383. <https://doi.org/10.4236/gep.2023.115022>.

38. Adeyeri OE, Akinsanola AA, Ishola KA (2017) Investigating surface urban heat island characteristics over Abuja, Nigeria: relationship between land surface temperature and multiple vegetation indices. *Remote Sens Appl Soc Environ* 7:57–68. <https://doi.org/10.1016/j.rsase.2017.06.005>
39. AlKafy A, Rahman MS, Alfaisal A, Hasan MM, Islam M (2020) Modelling future land use land cover changes and their impacts on land surface temperatures in Rajshahi, Bangladesh. *Remote Sens Appl Soc Environ* 18:100314. <https://doi.org/10.1016/j.rsase.2020.100314>
40. Mahmoud MI (2016) Integrating geoinformation and socio-economic data for assessing urban land-use vulnerability to potential climate-change impacts of Abuja, pp 1–256
41. Mumtaz F et al (2020) Modeling spatio-temporal land transformation and its associated impacts on land surface temperature (LST). *Remote Sens*. <https://doi.org/10.3390/RS12182987>
42. Kumi-Boateng B, Stemn E, Agyapong EA (2015) Effect of urban growth on urban thermal environment: a case study of Sekondi-Takoradi Metropolis of Ghana. *J Environ Earth Sci* 5(2):32–42
43. Aduah MS, Mantey S, Tagoe ND (2012) Mapping land surface temperature and land cover to detect urban heat island effect: a case study of Tarkwa, South West Ghana. *Res J Environ Earth Sci* 4(1):68–75
44. Hutcheson G (2011) Ordinary least-squares regression. *SAGE Dict Quant Manag Res*. <https://doi.org/10.4135/9781446251119.n67>
45. Firozjahi MK et al (2019) A PCA-OLS model for assessing the impact of surface biophysical parameters on land surface temperature variations. *Remote Sens*. <https://doi.org/10.3390/rs11182094>
46. Ghobadi Y, Pradhan B, Shafri HZM, Kabiri K (2015) Assessment of spatial relationship between land surface temperature and landuse/cover retrieval from multi-temporal remote sensing data in South Karkheh Sub-basin, Iran. *Arab J Geosci* 8(1):525–537. <https://doi.org/10.1007/s12517-013-1244-3>
47. Grover A, Singh R (2015) Analysis of Urban Heat Island (UHI) in Relation to Normalized Difference Vegetation Index (NDVI): A Comparative Study of Delhi and Mumbai. *Environments* 2(4):125–138. <https://doi.org/10.3390/environments2020125>
48. Environmental Systems Research Institute (ESRI), “Ordinary Least Squares (OLS) (Spatial Statistics),” 2013. .
49. Su S, Xiao R, Jiang Z, Zhang Y (2012) Characterizing landscape pattern and ecosystem service value changes for urbanization impacts at an eco-regional scale. *Appl Geogr* 34:295–305. <https://doi.org/10.1016/j.apgeog.2011.12.001>
50. Alibakhshi Z, Ahmadi M, Farajzadeh Asl M (2020) Modeling biophysical variables and land surface temperature using the GWR model: case study—Tehran and its satellite cities. *J Indian Soc Remote Sens* 48(1):59–70. <https://doi.org/10.1007/s12524-019-01062-x>
51. Li S, Zhao Z, Miaomiao X, Wang Y (2010) Investigating spatial non-stationary and scale-dependent relationships between urban surface temperature and environmental factors using geographically weighted regression. *Environ Model Softw* 25(12):1789–1800. <https://doi.org/10.1016/j.envsoft.2010.06.011>
52. Mensah E. Heat Island Effects in Tropical Sub Saharan City of Accra
53. Manu A, Twumasi Y, Coleman T (2006) Is it global warming or the effect of urbanization? The rise in air temperature in two cities of Ghana. *Ecosystem*
54. Zha Y, Gao J, Ni S (2003) Use of normalized difference built-up index in automatically mapping urban areas from TM imagery. *Int J Remote Sens* 24(3):583–594. <https://doi.org/10.1080/01431160304987>
55. Macarof P, Statescu F (2017) Comparasion of NDBI and NDVI as indicators of surface urban heat island effect in landsat 8 imagery: a case study of Iasi. *Present Environ Sustain Dev* 11(2):141–150. <https://doi.org/10.1515/pesd-2017-0032>
56. Stow DA et al (2016) Inter-regional pattern of urbanization in southern Ghana in the first decade of the new millennium. *Appl Geogr* 71:32–43. <https://doi.org/10.1016/j.apgeog.2016.04.006>
57. Agyemang FSK, Amedzro K, Silva E (2017) The emergence of city-regions and their implications for contemporary spatial governance: evidence from Ghana. *Cities* 71:70–79. <https://doi.org/10.1016/j.cities.2017.07.009>
58. Korah PI, Nunbogu AM, Akanbang BAA (2018) Spatio-temporal dynamics and livelihoods transformation in Wa, Ghana. *Land Use Policy* 77(May):174–185. <https://doi.org/10.1016/j.landusepol.2018.05.039>
59. Asabere SB et al (2020) Urbanization, land use transformation and spatio-environmental impacts: Analyses of trends and implications in major metropolitan regions of Ghana. *Land use policy* 96:104707. <https://doi.org/10.1016/j.landusepol.2020.104707>
60. Appiah DO, Forkuo EK, Bugri JT (2017) Land surface temperature extracts for peri-urban heat and rural cool troughs in Ghana. *Int J Adv Remote Sens GIS* 6(1):2204–2222. <https://doi.org/10.23953/cloud.ijarsg.274>
61. Nyamekye C, Kwofie S, Ghansah B, Agyapong E, Boamah LA (2020) Assessing urban growth in Ghana using machine learning and intensity analysis: a case study of the New Juaben Municipality. *Land Use Policy* 99:105057. <https://doi.org/10.1016/j.landusepol.2020.105057>
62. Ghimire B, Rogan J, Miller J (2010) Contextual land-cover classification: Incorporating spatial dependence in land-cover classification models using random forests and the Getis statistic. *Remote Sens Lett* 1(1):45–54. <https://doi.org/10.1080/01431160903252327>
63. Gislason PO, Benediktsson JA, Sveinsson JR (2004) Random forest classification of multisource remote sensing and geographic data. *Int Geosci Remote Sens Symp* 2(C):1049–1052. <https://doi.org/10.1109/igarss.2004.1368591>
64. Baboo DSS, Devi MR (2010) An analysis of different resampling methods in Coimbatore, District. *Glob J Comput Sci Technol* 10(15):61–66
65. Anderson JR (1976) A land use and land cover classification system for use with remote sensor data, vol 964. US Government Printing Office
66. Breiman L (2001) Random forests. *Random For*. <https://doi.org/10.1201/9780367816377-11>
67. Inglada J et al (2015) Assessment of an operational system for crop type map production using high temporal and spatial resolution satellite optical imagery. *Remote Sens* 7(9):12356–12379. <https://doi.org/10.3390/rs70912356>
68. Rodriguez-Galiano VF, Ghimire B, Rogan J, Chica-Olmo M, Rigol-Sanchez JP (2012) An assessment of the effectiveness of a random forest classifier for land-cover classification. *ISPRS J Photogramm Remote Sens* 67(1):93–104. <https://doi.org/10.1016/j.isprsjprs.2011.11.002>
69. Shade C, Kremer P (2019) Predicting land use changes in Philadelphia following green infrastructure policies. *Land* 8(2):28. <https://doi.org/10.3390/land8020028>
70. Gao BC (1996) NDWI a normalized difference water index for remote sensing of vegetation liquid water from space. *Remote Sens Env* 72:257–266

71. Lu Y, Feng X, Xiao P, Shen C, Sun J (2009) Urban heat island in summer of Nanjing based on TM data. *J Urban Remote Sens Event*. <https://doi.org/10.1109/URS.2009.5137628>
72. Herrmann SM, Anyamba A, Tucker CJ (2005) Recent trends in vegetation dynamics in the African Sahel and their relationship to climate. *Glob Environ Chang* 15(4):394–404. <https://doi.org/10.1016/j.gloenvcha.2005.08.004>
73. Chander G, Markham BL, Helder DL (2009) Summary of current radiometric calibration coefficients for Landsat MSS, TM, ETM+, and EO-1 ALI sensors. *Remote Sens Environ* 113(5):893–903. <https://doi.org/10.1016/j.rse.2009.01.007>
74. U.S. Geological Survey (2019) Landsat 8 Data Users Handbook. Nasa 8, 97
75. Van De Griend AA, Owe M (1993) On the relationship between thermal emissivity and the normalized difference vegetation index for natural surfaces. *Int J Remote Sens* 14(6):1119–1131. <https://doi.org/10.1080/01431169308904400>
76. Weisburd D, Piquero A (2008) How well do criminologists explain crime? Statistical modeling in published studies. *Crime Justice* 37:453–502. <https://doi.org/10.1086/524284>
77. Kleinbaum DG, Kupper LL, Muller KE, Nizam A (1998) Applied regression analysis and other multivariate methods. *J Mark Res* 15(3):498. <https://doi.org/10.2307/3150614>
78. Fotheringham AS, Brunsdon C, Charlton M (2002) Geographically weighted regression (the analysis of spatially varying relationships). Wiley, New York
79. Charlton M, Fortheringham S, Brunsdon C (2006) Geographically weighted regression, ESRC National Centre for Research Methods, NCRM Methods Review Papers 2005, NCRM/006
80. Eastman JR (2016) TerrSet Tutorial; Clark Labs. Clark University. Worcester, MA, USA
81. Agyapong EB, Ashiagbor G, Nsor CA, van Leeuwen LM (2018) Urban land transformations and its implication on tree abundance distribution and richness in Kumasi, Ghana. *J Urban Ecol* 4(1):1–11. <https://doi.org/10.1093/jue/juy019>
82. Chan JCW, Paelinckx D (2008) Evaluation of Random Forest and Adaboost tree-based ensemble classification and spectral band selection for ecotope mapping using airborne hyperspectral imagery. *Remote Sens Environ* 112(6):2999–3011. <https://doi.org/10.1016/j.rse.2008.02.011>
83. Shang X, Chisholm LA (2014) Classification of Australian native forest species using hyperspectral remote sensing and machine-learning classification algorithms. *IEEE J Sel Top Appl Earth Obs Remote Sens* 7(6):2481–2489. <https://doi.org/10.1109/JSTARS.2013.2282166>
84. Amoah A, Korle K (2020) Forest depletion in Ghana: the empirical evidence and associated driver intensities. *For Econ Rev* 2(1):61–80. <https://doi.org/10.1108/fer-12-2019-0020>
85. Tuffour-Mills D, Antwi-Agyei P, Addo-Fordjour P (2020) Trends and drivers of land cover changes in a tropical urban forest in Ghana. *Trees For People* 2:100040. <https://doi.org/10.1016/j.tfp.2020.100040>
86. Appiah DO, Schröder D, Forkuo EK, Bugri JT (2015) Application of geo-information techniques in land use and land cover change analysis in a peri-urban district of Ghana. *ISPRS Int J Geo-Information* 4(3):1265–1289. <https://doi.org/10.3390/ijgi4031265>
87. Braimoh AK, Vlek PLG (2004) Land-Cover Change Analyses in the Volta Basin of Ghana. *Earth Interact* 8(21):1–17. [https://doi.org/10.1175/1087-3562\(2004\)8%3c1:caitv%3e2.0.co;2](https://doi.org/10.1175/1087-3562(2004)8%3c1:caitv%3e2.0.co;2)
88. Ghana Statistical Service (GSS), “2010 Population & Housing Census National Analytical Report,” Ghana Stat. Serv., pp. 1–91, 2013, [Online]. Available: [http://www.statsghana.gov.gh/gssmain/fileUpload/pressrelease/2010\\_PHC\\_National\\_Analytical\\_Report.pdf%0Ahttp://statsghana.gov.gh/docfiles/2010phc/National\\_Analytical\\_Report.pdf](http://www.statsghana.gov.gh/gssmain/fileUpload/pressrelease/2010_PHC_National_Analytical_Report.pdf%0Ahttp://statsghana.gov.gh/docfiles/2010phc/National_Analytical_Report.pdf).
89. R. Grant, “Globalizing city: The urban and economic transformation of Accra, Ghana,” *Glob. City Urban Econ. Transform.* Accra, Ghana, pp. 1–187, 2009, doi: <https://doi.org/10.1080/00343400903132635>.
90. V. K. Quagraine, “Urban landscape depletion in the Kumasi metropolis. In: Adarkwa, K.K. (Ed.), *Future of the Tree: Towards Growth and Development of Kumasi*,” *Future Tree*, 2011, pp. 212–233, 2011.
91. Quayson A (2011) Housing affordability in Ghana: a focus on Kumasi and Tamale. *Ethiop J Environ Stud Manag* 3(3):1–11. <https://doi.org/10.4314/ejesm.v3i3.63958>
92. N. Boamah, “Housing Affordability in Ghana: A focus on Kumasi and Tamale,” *Ethiop. J. Environ. Stud. Manag.*, vol. 3, no. 3, 2011, doi: <https://doi.org/10.4314/ejesm.v3i3.63958>.
93. H. N. . Wellington, “Gated cages, glazed boxes and dashed housing hopes – In remembrance of the dicey future of Ghanaian housing.CSIR/GIA eds., *Proceedings of the 2009 National Housing Conference*,” Accra, Ghana, 2009. doi: <https://doi.org/10.1111/j.1747-1567.1988.tb02105.x>.
94. Afriyie K, Abass K, Adomako JAA (2014) Urbanisation of the rural landscape: Assessing the effects in peri-urban Kumasi. *Int J Urban Sustain Dev* 6(1):1–19. <https://doi.org/10.1080/19463138.2013.799068>
95. J. E. K. Akubia and A. Bruns, “Unravelling the Frontiers of Urban Growth : Spatio-Temporal Dynamics of Land-Use Change and,” pp. 1–23, 2019.
96. S. Malpezzi, A. G. Tiple, and K. G. Willis, “Cost and benefits of rent control in Kumasi, Ghana,” no. October, 1989.
97. K. B. Dickson, *A historical geography of Ghana*. CUP Archive, 1969.
98. Grant R, Yankson P (2003) Accra. *Cities* 20(1):65–74. [https://doi.org/10.1016/S0264-2751\(02\)00090-2](https://doi.org/10.1016/S0264-2751(02)00090-2)
99. Doan P, Oduro CY (2012) Patterns of population growth in peri-urban accra, ghana. *Int J Urban Reg Res* 36(6):1306–1325. <https://doi.org/10.1111/j.1468-2427.2011.01075.x>
100. R. Grant and J. Nijman, “Globalization and the Corporate Geography of Cities in the Less-Developed World,” *Ann. Assoc. Am. Geogr.*, vol. 92, no. 2, pp. 320–340, Apr. 2002, [Online]. Available: <http://www.jstor.org/stable/1515413>.
101. Cobbinah PB, Niminga-Beka R (2017) Urbanisation in Ghana: Residential land use under siege in Kumasi central. *Cities* 60:388–401. <https://doi.org/10.1016/j.cities.2016.10.011>
102. Guha S, Govil H, Dey A, Gill N (2018) Analytical study of land surface temperature with NDVI and NDBI using Landsat 8 OLI and TIRS data in Florence and Naples city, Italy. *Eur J Remote Sens* 51(1):667–678. <https://doi.org/10.1080/22797254.2018.1474494>
103. Adeyeri OE, Akinsanola AA, Ishola KA (2017) Remote Sensing Applications : Society and Environment Investigating surface urban heat island characteristics over Abuja, Nigeria : Relationship between land surface temperature and multiple vegetation indices. *Remote Sens Appl Soc Environ* 7(February):57–68. <https://doi.org/10.1016/j.rsase.2017.06.005>
104. Li Q, Lu L, Weng Q, Xie Y, Guo H (2016) Monitoring urban dynamics in the Southeast U.S.A. using time-series DMSP/OLS nightlight imagery. *Remote Sens* 8(7):13–15. <https://doi.org/10.3390/rs8070578>
105. Blake R et al (2011) Urban climate. In: Rosenzweig C, Solecki WD, Hammer SA, Mehrotra S (eds) *Climate Change and Cities*. Cambridge University Press, Cambridge, pp 43–82
106. Ranagalage M, Estoque RC, Murayama Y (2017) An urban heat island study of the Colombo Metropolitan Area, Sri Lanka, based on Landsat data (1997–2017). *ISPRS Int J Geo-Inf.* <https://doi.org/10.3390/ijgi6070189>
107. Zhou X, Wang YC (2011) Spatial-temporal dynamics of urban green space in response to rapid urbanization and greening



- policies. *Landsc Urban Plan* 100(3):268–277. <https://doi.org/10.1016/j.landurbplan.2010.12.013>
108. Malik MS, Shukla JP, Mishra S (2019) Relationship of LST, NDBI and NDVI using landsat-8 data in Kandaihimmat watershed, Hoshangabad, India. *Indian J Geo-Marine Sci* 48(1):25–31
109. Guha S, Govil H, Mukherjee S (2017) Dynamic analysis and ecological evaluation of urban heat islands in Raipur city, India. *J Appl Remote Sens* 11(3):1–23. <https://doi.org/10.1117/1.JRS.11.036020>
110. Guo G, Wu Z, Xiao R, Chen Y, Liu X, Zhang X (2015) Impacts of urban biophysical composition on land surface temperature in urban heat island clusters. *Landsc Urban Plan* 135:1–10. <https://doi.org/10.1016/j.landurbplan.2014.11.007>
111. Shu B, Zhang H, Li Y, Qu Y, Chen L (2014) Spatiotemporal variation analysis of driving forces of urban land spatial expansion using logistic regression: a case study of port towns in Taicang City, China. *Habitat Int* 43:181–190. <https://doi.org/10.1016/j.habitatint.2014.02.004>
112. Weng Q LRC (2005) Satellite remote sensing of urban heat islands: current practice and prospects. In: Jensen RR, Gatrell JD, McLean DD (eds) *Geo-spatial technologies in urban environments*. Springer, New York, pp 91–111
113. Xu H, Wen X, Ding F (2009) Urban expansion and heat island dynamics in the Quanzhou Region, China. *IEEE J Sel Top Appl Earth Obs Remote Sens* 2(2):74–79. <https://doi.org/10.1109/JSTARS.2009.2023088>
114. Estoque RC, Murayama Y, Myint SW (2017) Effects of landscape composition and pattern on land surface temperature: an urban heat island study in the megacities of Southeast Asia. *Sci Total Environ* 577:349–359. <https://doi.org/10.1016/j.scitotenv.2016.10.195>
115. Wilson JS, Clay M, Martin E, Stuckey D, Vedder-Risch K (2003) Evaluating environmental influences of zoning in urban ecosystems with remote sensing. *Remote Sens Environ* 86(3):303–321. [https://doi.org/10.1016/S0034-4257\(03\)00084-1](https://doi.org/10.1016/S0034-4257(03)00084-1)
116. Foody GM (2003) Geographical weighting as a further refinement to regression modelling: an example focused on the NDVI-rainfall relationship. *Remote Sens Environ* 88(3):283–293. <https://doi.org/10.1016/j.rse.2003.08.004>

**Publisher's Note** Springer Nature remains neutral with regard to jurisdictional claims in published maps and institutional affiliations.